

Assessing Potential Laser Strike Protection Engineering Control for United States Coast Guard Aircraft

Joe N. DeLauter

A thesis

Submitted in partial fulfilment of the
Requirements for the degree of

Master of Science

University of Washington

2016

Committee:

Mike Yost, PhD, MS

Marty Cohen, ScD, CIH, CSP

June Spector, MD, MPH

Program Authorized to Offer Degree:

Department of Environmental and Occupational Health Sciences

School of Public Health

©Copyright 2016

Joe N. DeLauter

University of Washington

Abstract

Assessing Potential Laser Strike Protection Engineering Control for United States Coast Guard Aircraft

Joe N. DeLauter

Chair of the Supervisory Committee:

Mike Yost, PhD, MS

Chair, Environmental and Occupational Health Sciences

Department of Environmental and Occupational Health Sciences

Background: There has been a tenfold rise in the number of reported laser strikes onto aircraft during the last decade; over 90% of which were caused by green lasers. Laser strikes on aircraft can cause a number of hazardous conditions for the crew, passengers, and people on the ground. Eye damage, such as flash blindness, loss of night vision, retinal lesions, or temporary/permanent blindness may occur, not to mention the possibility of skin burns or even crash landings.

Aim: This study assessed the viability of a thin film coating, specifically design to absorb/reflect green laser light as a potential engineering control to protect the people on-board the aircraft. Three factors were tested: the coatings ability to prevent green laser light transmission, the magnitude of glare production, and the magnitude of color distortion.

Methods: The light transmission of a green laser and a white light source through aircraft window test samples and a 532nm notch filter were measured by each light source's irradiance, radiant power, and light spectrum. Photographs of green laser strikes upon aircraft window test samples and a 532nm notch filter were analyzed via photographic software color histograms, comparing the magnitude of green light wavelengths to measure glare production. Photographs of various aircraft scenarios and a color reference card were used to analyze the magnitude of color distortion via photographic software color histograms of a white light source transmitting through the test samples and a 532nm notch filter.

Conclusions: Thin film coatings developed to reflect 532nm green laser light can be a very effective means to protect aircraft crews and passengers from the associated hazards of laser strikes. However, this engineering control is most effective when the laser beam is normal to the coated aircraft window. As the angle of incidence for the laser strike increases, the coating's effectiveness decreases. The thin film coating is also very effective in creating almost no glare when the laser beam is normal to the coated aircraft window, but produces a larger glare as the angle of incidence increases. Lastly, as the thin film coating reflects green light, it does not appear to greatly distort red and blue light intensities. Further research is needed to develop an engineering control designed to protect against laser strikes, such as a plexi-glass coating that can to shift the laser light away from the visual spectrum.

Table of Contents

Abstract.....	3
Background and Significance	6
Specific Aims	10
Methods.....	11
Results.....	15
Light Transmission	15
Glare Production.....	25
Color Distortion	33
Discussion and Conclusion.....	48
Limitations	54
Acknowledgments.....	55
Glossary.....	56
References	60
Appendixes.....	62

I. BACKGROUND AND SIGNIFICANCE

Since 2004, the Federal Aviation Administration (FAA) has been keeping track of an increasing hazard to the aviation community: laser strikes on aircraft. There were 384, 2836, and 3960 laser strikes reported in 2006, 2010, 2013 respectively, with an estimate of over 7100 for 2015. Each year since 2010, over 93% of cases reported being struck by green laser light according to the FAA, which released a spreadsheet in November 2015 containing information on all reported cases in the last five years (FAA 2015). To combat the rising number of laser strikes, the FAA and the Federal Bureau of Investigation (FBI) have joined together in tracking down those responsible and are imposing civil penalties of up to \$11,000 per violation, and in some cases \$30,800 for multiple strikes. The FAA has also implemented a media campaign to educate the public on the hazards of such actions. However, even with the increased civil penalties, public awareness videos, and FBI cooperation, the number of laser strike incidents continues to increase.

In December 2010, the Food and Drug Administration (FDA) limited consumer laser pointers to an energy output of 5mW (FDA 2010). However, more powerful lasers are becoming increasingly available due to online sales. Lasers above 5mW may cause flash blindness, loss of night vision, retinal lesions, temporary blindness, or even permanent blindness (FAA 2015). According to the FDA, even laser pointers of 5mW may become disruptive due to temporary flash blindness if directed at the eye during dark-adapted periods, such as night time flying. Figures 1 and 2 are laser strike simulations, and are good examples of how intense the laser light can be within the aircraft cockpit. Figure 3 illustrates how the eye focuses the laser's beam onto the fovea, where damage can occur due to the properties of the laser and duration of the exposure. Figure 4 displays damage caused by handheld laser pointers. The American National Standards Institute (ANSI), via the Laser Institute of America (LIA), created maximum permissible exposures (MPE) in the visual and near infrared regions of the energy spectrum (400nm – 1400nm) to prevent lesions from developing in the retina, the macula, and the fovea (ANSI 2014). ANSI recently updated their standards regarding laser safety with ANSI Z136.1-2014, and created the following classification structure for laser systems:

- Class 1 – Considered to be incapable of producing damaging radiation levels during operation, and exempt from any control measures.
- Class 1M – Considered to be incapable of producing hazardous exposure conditions during normal operation unless the beam is viewed with collecting optics and is exempt from any control measures other than to prevent potentially hazardous optically aided viewing.

- Class 2 – Emits in the visible portion of the spectrum (400 nm to 700 nm) and eye protection is normally afforded by the aversion response.
- Class 2M – Emits in the visible portion of the spectrum (400 nm to 700 nm) and eye protection is normally afforded by the aversion response for unaided viewing. However, Class 2M is potentially hazardous if viewed with collecting optics.
- Class 3R – Has reduced control requirements and is potentially hazardous under some direct and specular reflection viewing conditions if the eye is appropriately focused and stable, but the probability of an actual injury is small. This laser will not pose either a fire hazard or diffuse reflection hazard.
- Class 3B – May be hazardous under direct and specular reflection viewing conditions, but is normally not a fire hazard, diffuse reflection hazard, nor a laser generated air contaminant production hazard.
- Class 4 – Is a hazard to the eye or skin from the direct beam, may pose a fire hazard or diffuse reflection hazard, and may produce laser generated air contaminants and hazardous plasma radiation.

Although most classes of lasers may not present a hazardous condition, ANSI still recommends any person working around lasers to keep their exposures as low as possible. As mentioned in the class definitions, retinal damage is not the only form of a hazardous condition. Corneal damage, skin burns, laser generated air contaminants, and fires are also associated with laser light exposure, depending on the laser's intensity (ANSI 2014). Furthermore, when lasers are pointed at aircraft cockpits, the hazard not only affects the eyes of the aircrew, but also puts the safety of any passengers or people on the ground into question. As mentioned above, the FDA has limited private-use handheld lasers to 5mW, which are classified as Class 3R. However, Class 3B and even Class 4 lasers are still being used to strike aircraft and other modes of transportation. In October 2015, a Washington State Ferry was struck by a Class 4 blue 5W laser, where one of the ferry captains suffered skin burns on their eyelids (Bush 2015).

Since the 1970's, several organizations have been developing laser protection methods, which include eyewear, reflective mirrors or glass, and light filters; each control designed for a specific range of wavelengths and intensities. However, since eyewear is designed for a specific range of wavelengths, the eyewear is always heavily tinted and may reduce visibility. This is a problem for aircrews, whose eyes cannot afford to lose any visibility. Aircrews depend on different colored lights on the ground and in the air, especially at night, to perform different maneuvers. Arguably the most important maneuver is landing, where laser strikes have increased on aircraft below 2000ft from 12.5% of reported cases to

26.7% between 2004 to 2008 (Nakagawara 2011). Crewmembers could become distracted at that altitude, or suffer from an afterimage, thus increasing the risk of a crash landing. Yet, Marshall et al. states that no aircraft have actually crashed due to laser strikes, nor have there been any reports of crewmembers suffering from permanent retinal damage due to laser strikes (Marshall 2016). However, as the number of laser strikes continues to increase, it may be only a matter of time until a crewmember is seriously injured from a laser strike, such as with the ferry captain.

Other operations that cannot afford to have any loss of visibility are search and rescue, drug and migrant interdictions, and law enforcement. The United States Coast Guard (USCG) performs all of these missions and more, and is no stranger to laser strikes. Figures 5 and 6 are two examples of USCG aircraft that have experienced laser strikes. It is currently updating its policies on how to deal with laser strikes, and has been improving its pilot training program to include laser strike protection procedures. However, due to the nature of USCG search and rescue operations, no tinted or colored eyewear or glass are allowed to be used to protect pilots for laser strikes. According to LCDR James Cooley of USCG AIRSTA Astoria, an engineering control, such as a thin film coating, would be ideal for the aircraft as a protective measure, so that it may be applied during manufacturing and the pilots do not have to worry about it during flight operations. Therefore, the purpose of this study was to identify and test a window coating designed specifically to target green laser wavelengths (532nm) without substantial color distortion by the plexi-glass windows or reduction in operational effectiveness of the crew.



Figure 1: a demonstration by the USCG to show just how disruptive to the visibility and night vision of pilots laser pointers can be (Negroni 2013).



Figure 2: a demonstration of a laser strike during the landing of a commercial jet in a flight simulator (Negroni 2013).

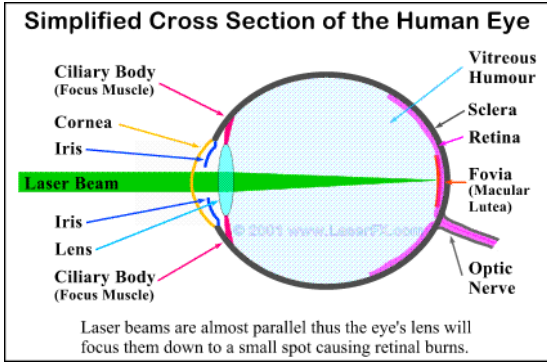


Figure 3: Illustration of laser striking the fovea (LaserFX 2008)

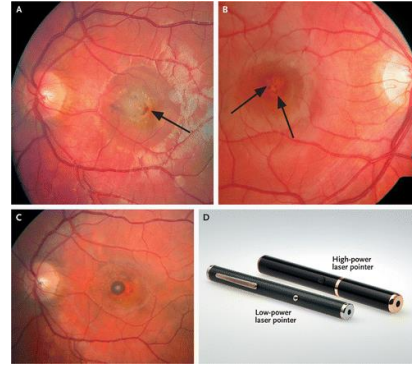


Figure 4: Eye damage caused by a laser pen (Wyrsh 2010)



Figure 5: the USCG MH-60 Jayhawk



Figure 6: the USCG MH-65 Dolphin

II. SPECIFIC AIMS

USCG aircrews are subjected to a variety of hazardous conditions during operations. One of the least addressed has been the threat of a laser strike. Laser strikes can occur instantly at any time, and may cause flash blindness, loss of night vision, retinal damage, skin burns, temporary blindness, or even permanent blindness. Several forms of personal protective equipment exist, though none offer protection without a reduction in clear visibility. Since USCG operations are often life or death situations, a loss in visibility is not an option. To minimize the hazard of laser strikes, a new engineering control must be developed. This study is designed to test a combination of laser protection techniques with lens filtration technologies and investigate the feasibility of a coating for aircraft windows that specifically prevents green laser light from causing hazardous conditions within the aircraft cockpit. To determine whether there is a better engineering control than personal protective equipment, the specific aims of this study were:

1. To determine the change in light transmission with the application of a thin film coating that absorbs/reflects 532nm laser light at 90mW.
Null hypothesis: the 532nm notch filter will transmit >5mW of 532nm laser light.
Alternate hypothesis: the 532nm notch filter will not transmit >5mW of 532nm laser light.
2. To determine the change in glare production with the application of a thin film coating that absorbs/reflects 532nm laser light at 90mW.
Null hypothesis: the 532nm notch filter will not produce less glare when struck by a 532nm laser at 90mW.
Alternate hypothesis: the 532nm notch filter will produce less glare when struck by a 532nm laser at 90mW.
3. To determine the amount of color distortion with the application of a thin film coating that absorbs/reflects 532nm laser light at 90mW.
Null hypothesis: the 532nm notch filter will visibly distort the color of light transmitted.
Alternate hypothesis: the 532nm notch filter will not visibly distort the color of light transmitted.

The results of this study will be directly applicable for use by the USCG to determine if the developed aircraft window coating will be a viable engineering control for the prevention of hazardous conditions brought on by green laser strikes. In addition, this study was to determine if the developed aircraft window coating will be able to still allow the vast majority of white light to transmit and provide the clearest visibility possible. Finally, this study will help pave the way for more improved window coatings not only for the USCG, but the entire aviation community, and for coatings that prevent multiple types of laser light (green, red, and/or blue) from creating hazardous conditions. Experiments like this one have been done in the past; however, very few have tried to combine laser protection techniques and lens filtration technology to be used on the aircraft windows.

III. METHODS

This study compared the light transmission, glare production, and color distortion characteristics of uncoated test samples and one coated test sample. The uncoated test samples were sixteen 2x2in pieces cut from a used plexi-glass window (Figure 7) from a USCG MH-65C Dolphin (Figure 6) to act as uncoated test samples. The 16 pieces (Figure 9) were stacked on top of each other to determine which were the flattest and which had the largest relative curvature. The three flattest test samples were determined to be TS 2, TS 3, and TS 4, and the three test samples with the largest curve were determined to be TS 13, TS 14, and TS 16. Those six pieces were compared to an off-the-shelf notch filter (532NF) with a thin film coating specifically designed to absorb/reflect $532\pm 13.3\text{nm}$ wavelengths at an optical density of 4 (Figure 8). All data was collected in a light-tight test chamber (Figure 10). See Appendix B for full methodology procedures.

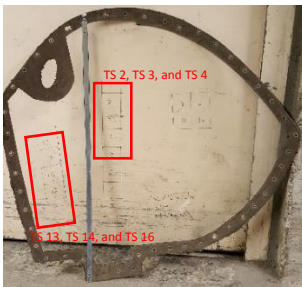


Figure 7: USCG MH-65C Dolphin plexi-glass window

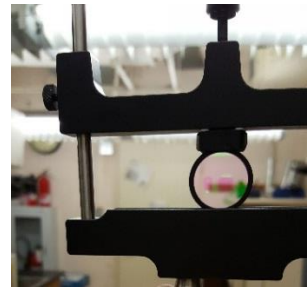


Figure 8: 532nm, OD 4 notch filter

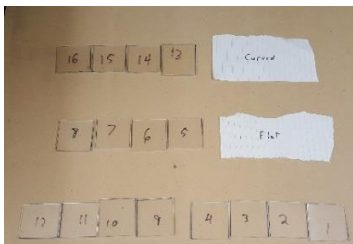


Figure 9: the 16 uncoated test samples



Figure 10: testing chamber

A. Light Transmission

For the light transmission measurements, each test sample was struck by a 532nm, 90mW laser as the laser light source and a collimated halogen bulb as the white light source (WLS) at a 00° and a 60° angle of incidence. The following equipment was mounted on a 2.0m optical rail: the light source, followed by the test sample, then neutral density filters (if needed), and finally a spectrometer. The convex side of the curved test samples faced the light source. Neutral density filters, with optical densities of 2.5 and 0.9, were used to evenly knock down the amount of laser light being transmitted to the spectrometer; otherwise, the laser would have overloaded the spectrometer's sensor. The neutral density filters were not necessary for measurements involving the WLS. The spectrometer was chosen as the measuring

device because it was capable of measuring the light source's spectrum (approx. 190-1110nm) in units of absolute irradiance (W/cm^2), which were then used to calculate the light source's percent transmission (%) and the radiant power (W) per test sample.

Prior to each light transmission measurement, the test samples were cleaned in accordance with lens cleaning procedures in Appendix A. Once the optical rail was setup in accordance with Appendix B, a dark spectrum was first taken with no light source activated within the test chamber, followed by a spectrum measurement of the light source activated with no test sample. Then test samples were struck one at a time by the laser at a 00° angle of incidence, then at a 60° angle of incidence. Each spectrum was measured at a distance of 0.5m from the light source to the test sample, with the spectrometer's sensor 0.7m from the light source. Once all test sample spectrums per angle of incidence were measured, the laser was replaced by the white light source. Each test sample was struck by the WLS at a 00° and a 60° angle of incidence, again at a distance of 0.5m from the light source to the test sample and 0.7m to the spectrometer sensor. Upon completion of the WLS spectrum measurements per test sample per angle of incidence, the 532NF was struck by the WLS at 00° , 10° , 20° , 30° , 40° , 50° , and 60° angles of incidence to determine the characteristics of a shift in the notched portion of the visual spectrum.

Each spectral reading was saved in SpectraSuite in units of absolute irradiance. The data was copied into Excel, where it was corrected for the neutral density filters and used to calculate the percent transmission and radiant power. The 2.5 and 0.9 neutral density filters only allowed for 0.0398% of the test samples' transmitted laser light to transmit to the spectrometer's sensor; therefore, the absolute irradiance per wavelength had to be divided by 3.98×10^{-4} to provide a corrected absolute irradiance. Then each test sample's absolute irradiance was divided by the light source's absolute irradiance to calculate the percent transmission of light per wavelength.

To calculate radiant power, the absolute irradiance was multiplied by the surface area of the spectrometer's sensor per test sample per wavelength. Since the beam of the laser was slightly inside the spectrometer sensor's diameter, 100% of the laser's radiant power was experienced by the spectrometer's sensor; therefore, the absolute irradiance is equal to the radiant power. The WLS's beam diameter was much larger than the surface area of the spectrometer's sensor; therefore, the absolute irradiance was multiplied by sensors surface area of $0.1149cm^2$.

B. Glare Production

Only the laser was used as a light source for the glare production measurements. This section was to simulate a crewmember being exposed, not to the laser beam itself, but to the glare produced by the

laser beam onto the aircraft window. Lasers can produce a lot of glare on windows and is the second most hazardous condition crewmembers experience (after direct eye exposure); see Figures 1 and 2. In accordance with Appendix B, the optical rail was setup within the test chamber similarly to the light transmission measurements; however, the spectrometer was replaced by a camera. The camera was placed 1.2m away from the laser, with the laser's beam aligned to 1.0mm below the aperture. This was so the laser did not overload the camera, but have the camera experience as much light intensity as possible on a near axis alignment.

Prior to each picture taken by the camera, the test samples were cleaned in accordance with Appendix A. A picture was first taken without the laser being activated, followed by a picture of the laser striking the camera without a test sample. Then each test sample was struck by the laser in turn at a 00° and a 60° angle of incidence at a distance of 0.5m from the laser.

The pictures were loaded into ImageJ to measure the amount of pixels per intensity level for the color green and in grayscale. The picture with no laser light was used as a blank, so as to exclude any background color the camera may detect without light. This was to provide a much better comparison of the laser light with no test sample to the 532NF and the uncoated test samples. The photographic software did not detect any pixels above a green intensity level of 17 for the no test sample, so all test sample histograms measured pixels above an intensity level of 17. Each picture's histogram was copied into Excel, where the cumulative percentages of pixels per intensity level were calculated. The intensity levels at the 15% and 95% cumulative percentiles were used to calculate the contrast ratio per test sample. Then the contrast ratio and the intensity levels at the 25%, 50%, and 75% cumulative percentiles were tabulated to calculate the p-values comparing the flat vs the curved test samples and the 532NF vs all of the window test samples.

C. Color Distortion

For the color distortion measurements, a slide projector was used as the WLS. In accordance with Appendix B, a 1.0m optical rail was setup with the slide projector next to and below the camera to illuminate a scenario photograph. The camera was at a 00° angle of incidence at a distance of 0.2m to the scenario photograph to prevent the camera from automatically focusing or zooming. The scenario photograph was angled at 65° to prevent a glare, produced by the WLS, from showing up in the picture taken by the camera. Prior to each picture taken by the camera, the test samples were cleaned in accordance with Appendix A. All scenario photographs had a picture taken of it without any test sample on the camera taken first, followed by pictures with each test sample taped over the camera's aperture to simulate a crewmember looking through the aircraft window onto the scenario.

Assessing Potential Laser Strike Protection Engineering Control for United States Coast Guard Aircraft

The pictures were loaded into ImageJ to create histograms for the colors green, red, and blue. The picture with no laser light was again used as a blank, all test sample histograms were measured above a green intensity level of 18, a red intensity level of 20, and a blue intensity level of 21. Each picture's histogram was copied into Excel, where the 25%, 50%, and 75% cumulative percentages of pixels per intensity level were calculated and tabulated. The intensity levels at the 15% and 95% cumulative percentages were used to calculate the contrast ratio per test sample.

IV. RESULTS

1. Light Transmission

A. Laser spectral data at 00°

i. Absolute irradiance

Absolute irradiance was the unit of measure provided by the spectrometer in units of mW/cm², in accordance with the spectrometer's operating procedures in Appendix D. The laser's peak absolute irradiance was roughly 90mW/cm² at approximately 532.5nm. This means that the laser is not centered exactly at 532nm, but is still within the manufacturer's ±1.0nm operational limits. The absolute irradiance was then calculated into radiant power as described in the "Methods" section.

ii. Radiant power

Radiant power graphs were included to illustrate how power is attenuated by the 532NF when compared to the uncoated test samples. Since radiant power is used by ANSI to determine laser classes, it was important to see if the 532NF could reduce the radiant power to safe levels. For the purposes of this study, a hazardous condition exists when more than 5.06 mW of green laser light radiant power was detected through the test sample:

Assumptions:

t = human eye aversion response time = 0.25s

worst case pupil dilation for night vision = 8.0mm diameter

Calculations:

ANSI Maximum Permissible Exposure of a laser beam at 532nm for 5*10⁻⁶s to 10s =

$$1.8t^{0.75} * 10^{-3} \text{J} * \text{cm}^2 = 1.8 * (0.25)^{0.75} * 10^{-3} = 6.36 * 10^{-4} \text{J} * \text{cm}^2$$

$$6.36 * 10^{-4} / 0.25 = 2.55 * 10^{-3} \text{W} * \text{cm}^2$$

$$\text{surface area of eye exposed} = \pi * (8/2)^2 = 50.3 \text{mm}^2 = 0.503 \text{cm}^2$$

$$2.55 * 10^{-3} / 0.503 = 0.00506 \text{W} = \mathbf{5.06 \text{mW}}$$

For a 90mW laser, the uncoated test samples were only able to reduce the radiant power on average 10-20%, between 65-80mW. According to the FDA, even 5mW could cause flash blindness; therefore, the uncoated test samples are not able to attenuate the radiant power of the laser on their own, which was expected. Due to the effectiveness of the 532NF at a 00° angle of incidence, it was not easy to see the 532NF's absolute irradiance in Figure 11; therefore, a zoomed in graph is shown in Figure 12. The 532NF specifications indicated an optical density of 4.0, which means that only 0.009mW/cm², or 0.01%, of the laser was supposed to transmit through it. According to Figure 12, just above 0.0006mW (6.67*10⁻⁴%) of the laser light transmits, which suggests that the 532NF's actual optical density is closer

to 5.18. The manufacturer does state that the optical density may be greater than 4. The neutral density filters were not used to measure the 532NF's spectrum at a 00° angle of incidence, meaning that there is no gain in optical density due to unit correction calculations. A maximum radiant power just above 0.0006mW for the 532NF is well below the 5mW safety level set by the FDA for personal use lasers and ANSI for Class 3R lasers.

This graph also shows that all of the uncoated test samples more or less follow the same spectrum as the laser. Although, the differences between the uncoated test samples in Figure 9 may be due to several factors, such as surface scratches, manufacturing imperfections, or different thicknesses of material.

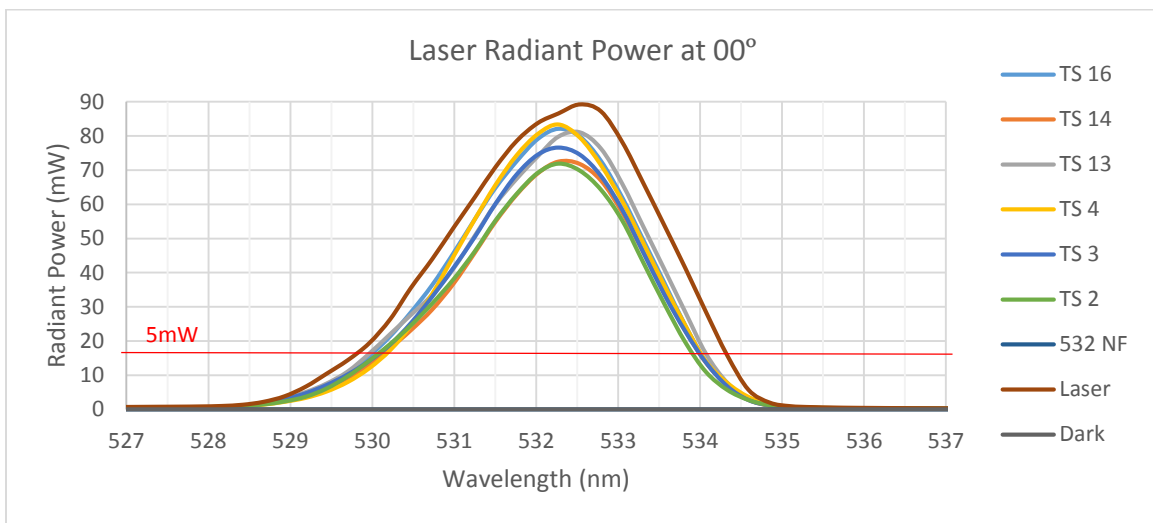


Figure 11: Laser spectrum radiant power per wavelength for all test samples at 00° (corrected for neutral density filters)

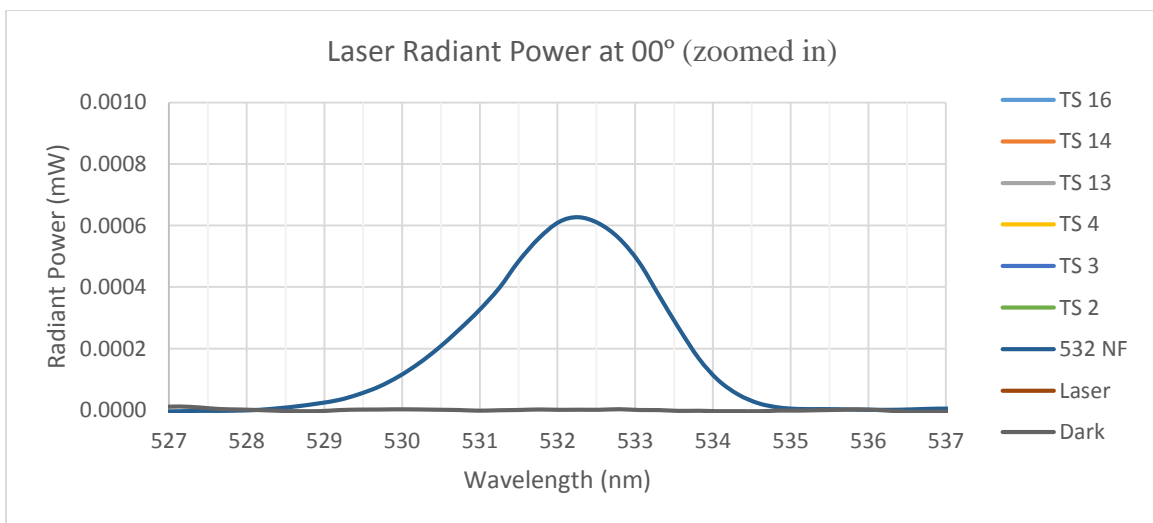


Figure 12: Laser spectrum radiant power per wavelength for all test samples at 00° (corrected for neutral density filters)

iii. Percent transmission

Percent transmission graphs were included, because it is an easy way to see the magnitude of light transmission reduction by the test samples, and determine the difference in the amount of green light transmitted by the 532NF compared to the uncoated test samples. The laser's spectrum (with no test sample) was assumed to be the maximum amount of light able to transmit to the spectrometer's sensor; thus a ratio of the test sample data over the laser's data was used to calculate the percent transmission.

Again, Figure 13 shows that the uncoated test samples follow a similar pattern across the spectrum. The most amount of light transmitted is at the laser's centered wavelength of 532nm. The two dips at 529nm and 534nm occur because the uncoated test samples reach lower levels of absolute irradiance before the laser does, so the percentage of transmitted light decreases until they begin to equal each other again outside of 527-537nm.

Figure 13 also clearly indicates just how little laser light is transmitted through the 532NF when compared to the uncoated test samples, because the 532NF's percent transmission on the graph shown is undetectable. Therefore, another zoomed in graph is provided; Figure 14. Unlike the uncoated test samples, the percent transmission for the 532NF is not as dramatic between 529nm and 535nm; it is roughly flat with no large dips. The rise in percent transmission at 537nm means that the 532NF's and the laser's absolute irradiances are starting to decrease together, and will eventually be fairly equal as they reach the edges of the visual spectrum.

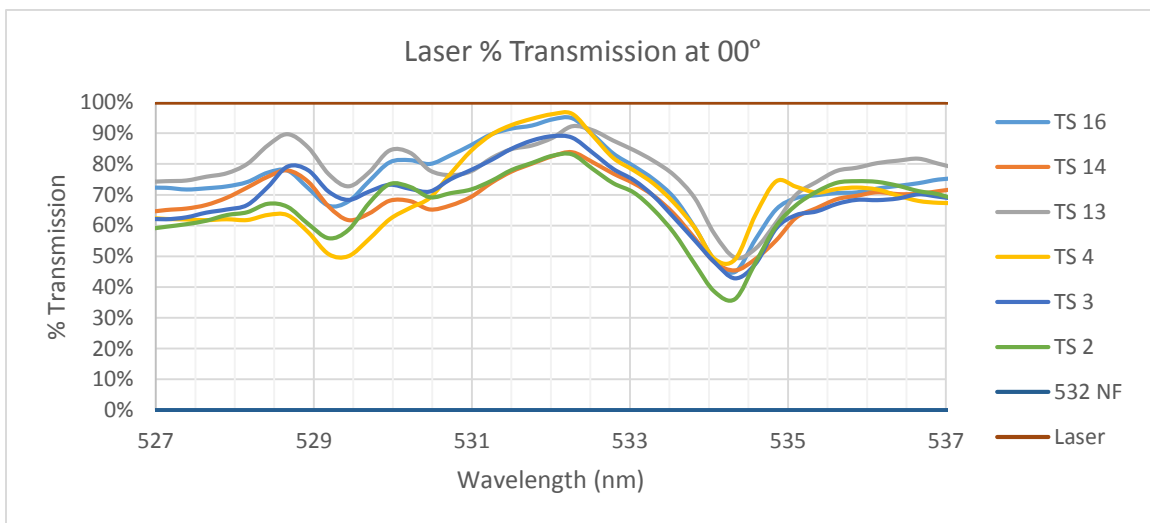


Figure 13: Laser spectrum percent transmission per wavelength for all test samples at 00°

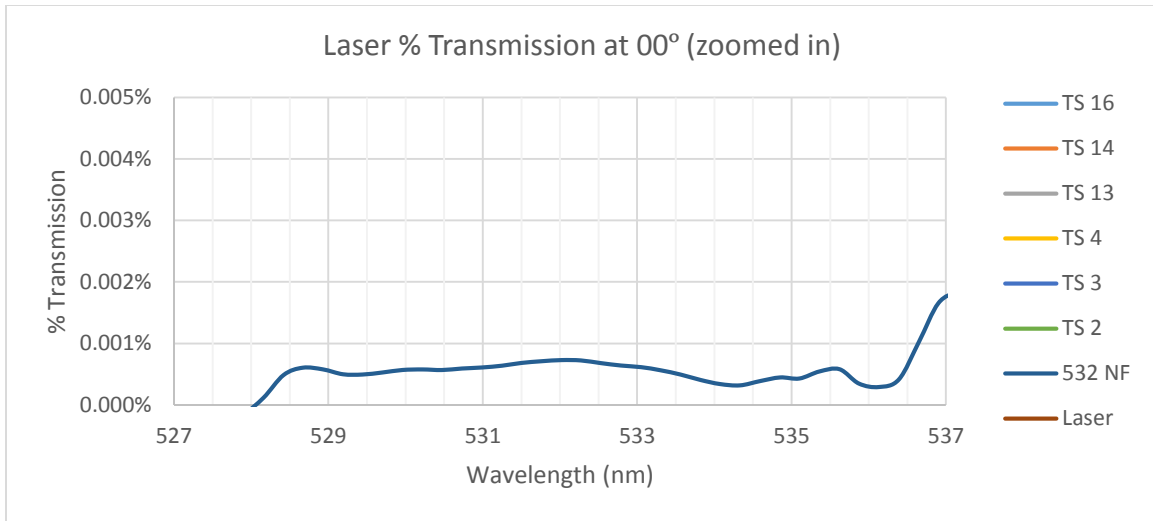


Figure 14: Laser spectrum percent transmission per wavelength for all test samples at 00°

B. Laser spectrum data at 60°

i. Absolute irradiance

At a 60° angle of incidence, Figure 15 indicates that the magnitude of absolute irradiance through the uncoated test samples is reduced 55%-80%; whereas, at 00° the reduction was only 10%-20%. The reason for this extra reduction is due to more light being reflected off the surface of the uncoated test samples, as well as the increase in material the laser’s beam has to travel through causing the light to refract more away from the spectrometer’s sensor. Although the uncoated test samples have reduced their absolute irradiances to less than half of the laser’s, the 532NF absolute irradiance has increased from a 0.0006mW/cm² to approximately 25.0mW/cm², and doesn’t provide any more protection than that of the uncoated samples. Another interesting takeaway from Figure 15 is that the three flat uncoated test samples may be better at reducing the absolute irradiance of the laser than the three curved test samples. The three flat uncoated samples appear to reduce the laser’s absolute irradiance by 75%-80%, but the curved uncoated test samples only reduce the laser’s absolute irradiance by 60%-70%.

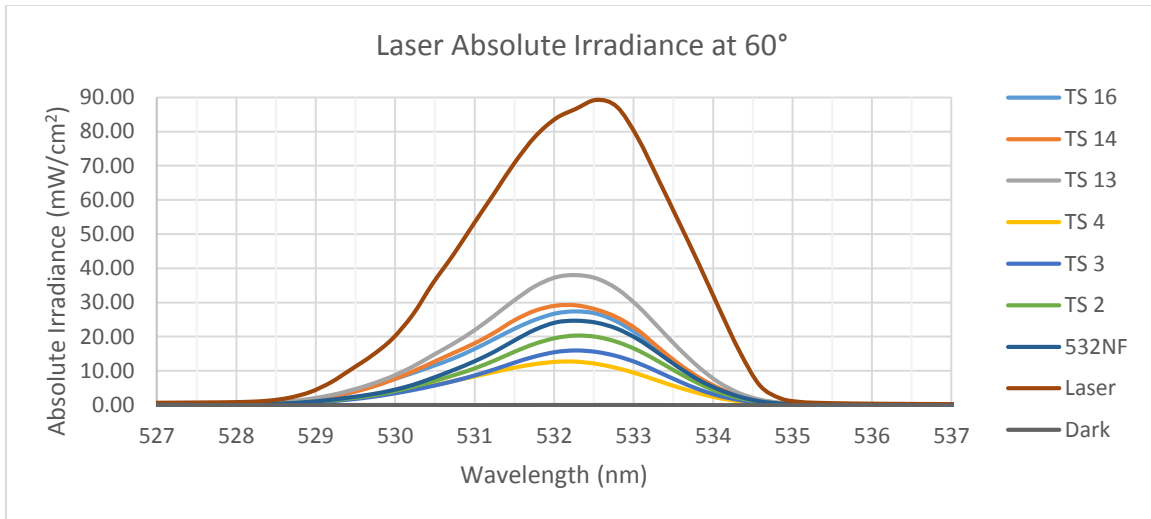


Figure 15: Laser spectrum absolute irradiance per wavelength for all test samples at 60° (corrected for neutral density filters)

ii. Radiant power

Figure 16 presents the laser’s radiant power transmitted through the test samples at a 60° angle of incidence. This graph indicates that the uncoated test samples are still not providing enough protection against a 90mW laser, and now neither is the 532NF. The uncoated test samples were able to reduce the 90mW amount of radiant power down to 15-40mW, but is still 5-8 times higher than safe levels. Even the 532NF is 5 times higher than safe levels at 25mW of radiant power transmitted. This implies that as the angle of incidence increases, the 532NF becomes much less protective against the hazardous conditions of a laser strike.

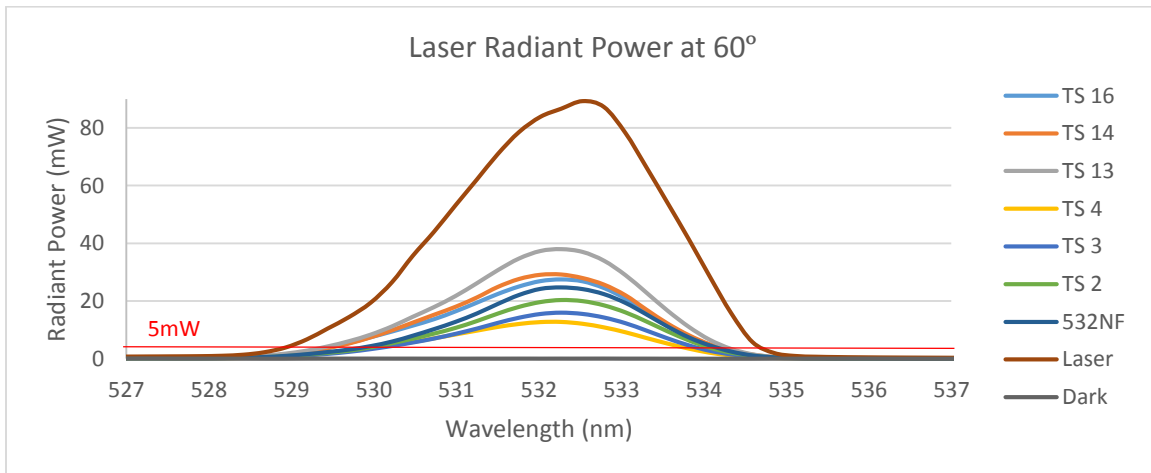


Figure 16: Laser spectrum radiant power per wavelength for all test samples at 60° (corrected for neutral density filters)

iii. Percent transmission

Figure 17 illustrates the percent of light transmitted by the laser through the test samples at a 60° angle of incidence. Unlike at a 00° angle of incidence, all of the test samples are fairly even across the spectrum and follow the same pattern, and transmit at much lower percentages than at 00°. This

graphs also indicates that the flat uncoated test samples may be better at attenuating the laser light better than the curved uncoated test samples, because each flat test sample is below the curved ones. It is possible that during the manufacturing process the flatter portions of the window are thicker than the curved portions; the thicker material scatters more of the laser light, thus placing their spectrum further down the y-axis of Figure 17.

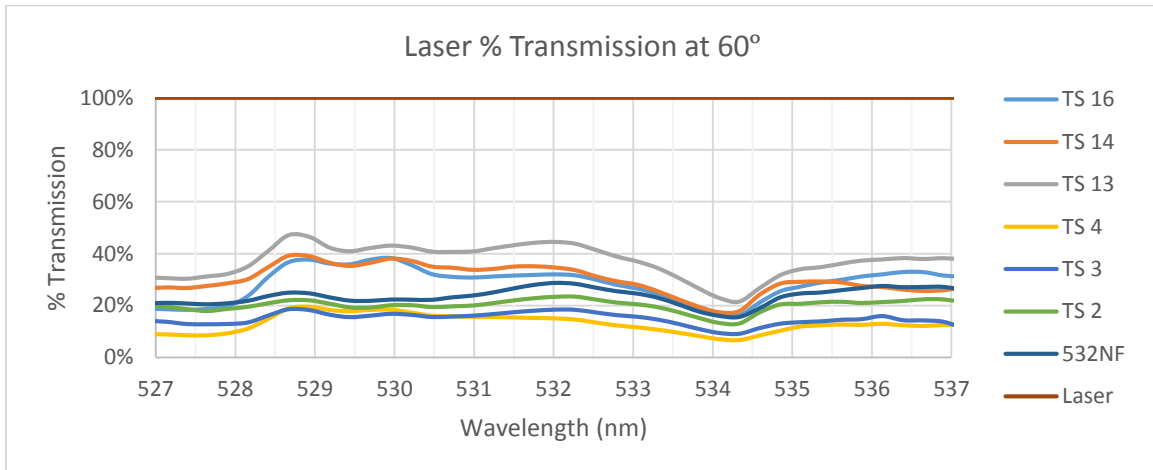


Figure 17: Laser spectrum percent transmission per wavelength for all test samples at 60° (corrected for neutral density filters)

C. White light source spectrum data at 00°

i. Absolute irradiance

As with the laser transmission graphs, the WLS x-axis is the wavelength, but labeled over the entire visual spectrum, as was desired with a white light source (a graph of the broad spectrum). The previous graphs of the laser only showed 527-537nm, because the only light source was the laser (centered at 532nm) and the rest of the spectrum had negligible readings. The WLS, however, has wavelengths throughout the visual spectrum, and therefore shows that the 532NF only decreases the amount of green laser light, allowing the rest of the spectrum to transmit through the material. Figure 18 displays the 532NF doing what it is designed to do; reflect 532±13.3nm. The 532NF filters out less of the WLS than the other test samples. The closer to the full absolute irradiance of the WLS, the more white light that could enter the aircraft cockpit without scattering or reflecting, allowing the pilots clearer visibility. Although, the uncoated test samples do not transmit the full amount of absolute irradiance per wavelength, all six are relatively at the same level.

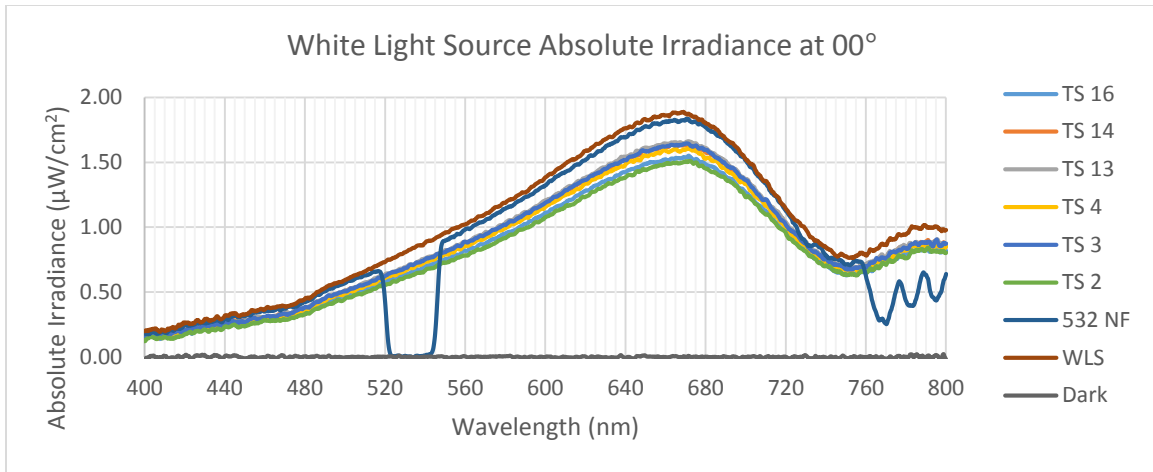


Figure 18: WLS spectrum absolute irradiance per wavelength for all test samples at 00°

ii. Radiant power

The radiant power of the WLS at a 00° angle of incidence is shown by Figure 19. The radiant power for the WLS is over a thousand times smaller than the radiant power of the laser, which was expected.

Halogen bulbs do not transmit nearly as much radiant power as the laser used in this study.

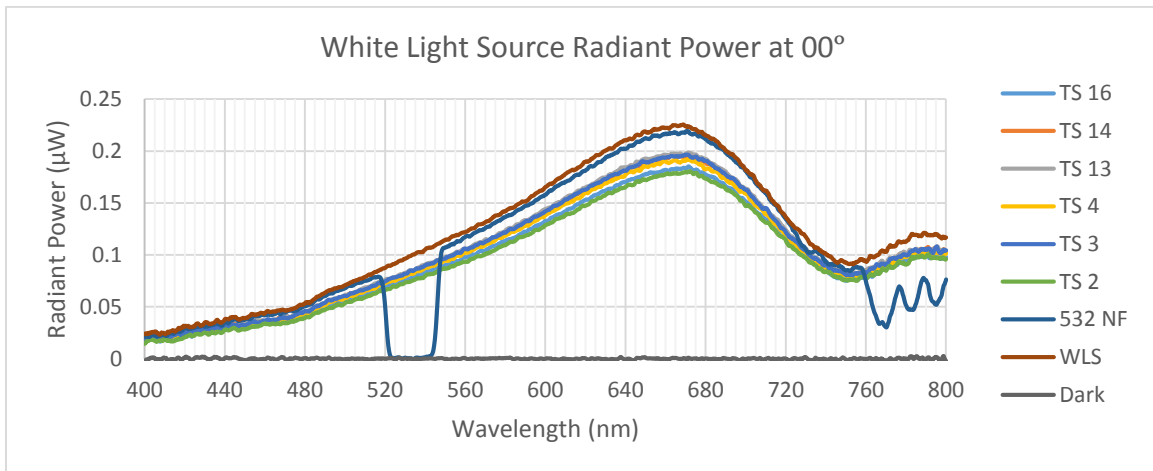


Figure 19: WLS spectrum radiant power per wavelength for all test samples at 00°

iii. Percent Transmission

Figure 20 is the percent transmission of the WLS at a 00° angle of incidence. This graph is an easier way to see that the 532NF indeed allows most of the white light to transmit, except at $532 \pm 13.3 \text{ nm}$; whereas the uncoated test samples only allow through 65%-85% of the white light. Some possibilities as to why the uncoated test samples are not closer to 100% white light transmission could be surface imperfections such as scratches, or they refract/reflect more white light than the 532NF due to its molecular composition (polymer vs glass), or the uncoated test samples could have their own type of coating applied during its manufacturing.

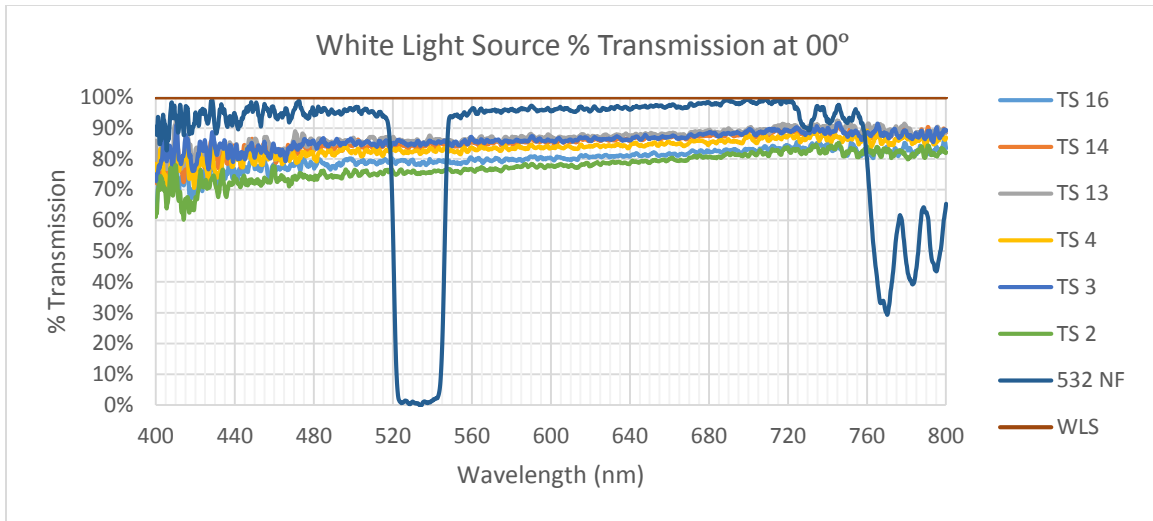


Figure 20: WLS spectrum percent transmission per wavelength for all test samples at 00°

D. White light source spectrum data at 60°

i. Absolute irradiance

Figure 21 shows the WLS spectrum with a 60° angle of incidence between the WLS and the test sample. Just as with the laser at a 60° angle of incidence, the absolute irradiance of the WLS is reduced by all test samples, including the 532NF, by about 40%-50%. This decrease may be due to more material to transmit through or refracting and reflecting more light away from the spectrometer’s sensor. Also, the 532NF’s notched portion of the spectrum has shifted from 532nm (the wavelength it was design to reflect) to 460-470nm. This may be due to the notch filter not reflecting light properly when the light strikes the 532NF; therefore, there would be less reflected light interfering with non-reflected light.

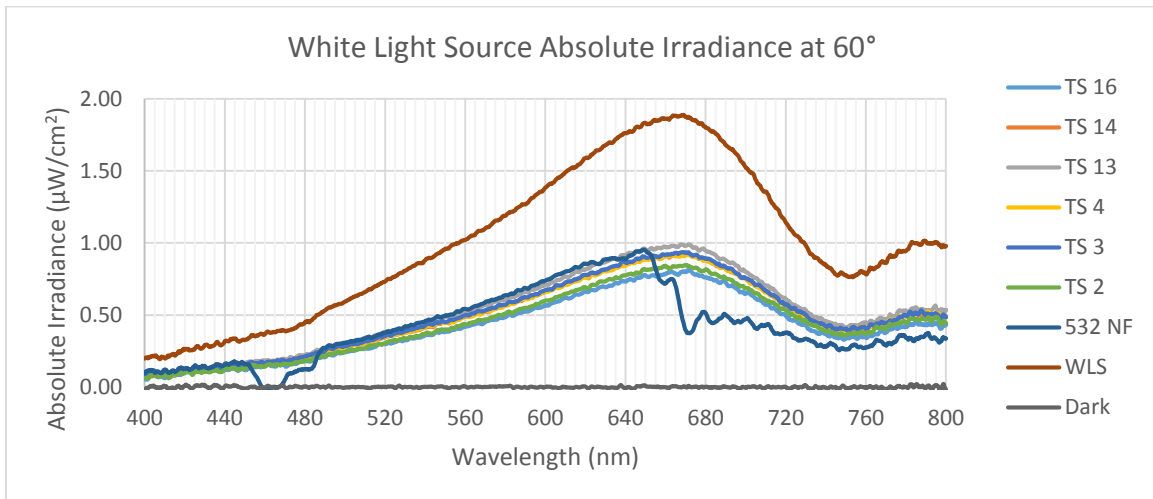


Figure 21: WLS spectrum absolute irradiance per wavelength for all test samples at 60°

ii. Radiant power

Figure 22 displays the radiant power of the WLS at and at a 60° angle of incidence. The radiant power for the WLS is over a thousand times smaller than the radiant power of the laser, which was expected. This graph again shows the additional attenuation of white light with a 60° angle of incidence.

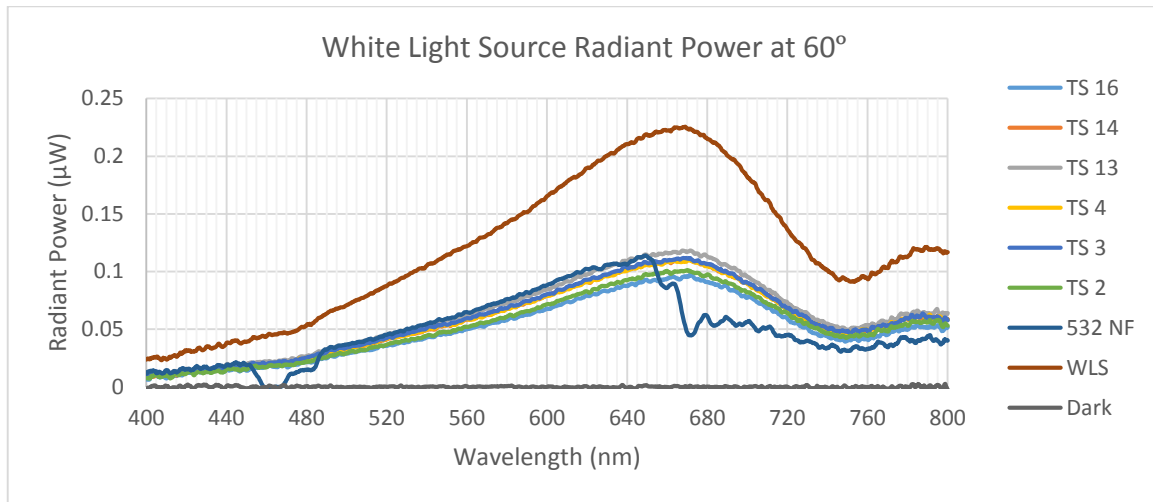


Figure 22: WLS spectrum radiant power per wavelength for all test samples at 60°

iii. Percent transmission

Figure 23 shows the percent transmission of the WLS through the tests samples at a 60° angle of incidence. For all the test samples, the percent transmission decreases from 65%-85% at 00° angle of incidence to 40-50% at 60° angle of incidence. Furthermore, the 532NF has a much narrower range to which most it is the most optimal at transmitting white light. It is the least optimal at transmitting white light between 450-485nm due to the shift in its notched portion of the spectrum as displayed in Figure 23, but is also the least optimal after 665nm. After 665nm, the 532NF produces an etalon, where the white light is being reflected back and forth between the layers of the thin film coating, causing the light to scatter away from the spectrometer’s sensor. This is why the percent transmission is so much lower within the etalon. Each peak of the etalon could be a layer of that thin film coating.

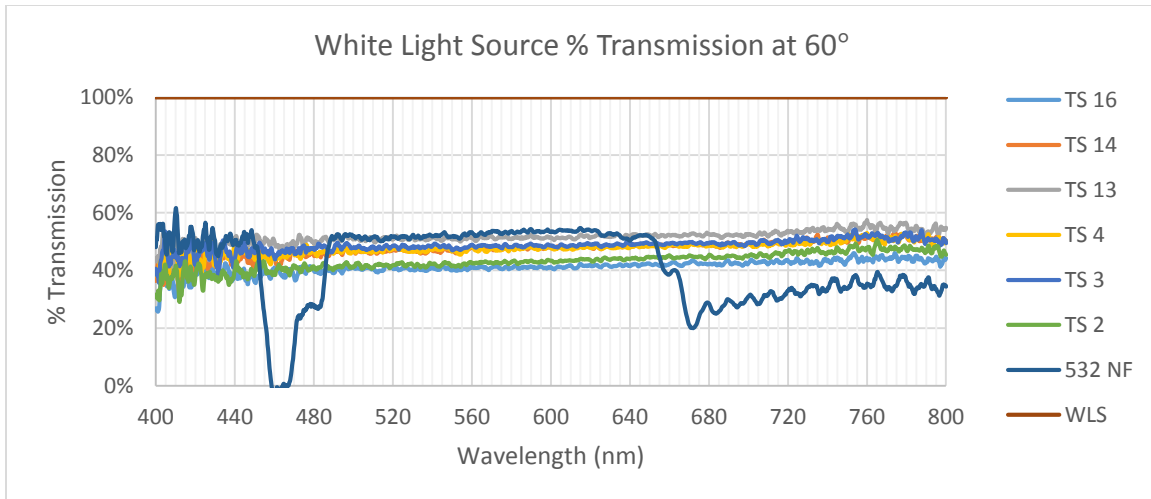


Figure 23: WLS spectrum percent transmission per wavelength for all test samples at 60°

E. Spectrum notch shift per angle of incidence for 532nm notch filter

Figure 24 is a graphical representation of the 532NF’s notched portion of the visual spectrum shifting as the angle of incidence increases. At a 00° angle of incidence, the 532NF is doing what it was designed to do, absorbing/reflecting 532±13.3nm. The notched portion of the spectrum moves approximately 5-15nm to the left with every 10° angle of incidence increase. At a 30° angle of incidence though, a step starts to show in the notched portion of the spectrum. Every 10° increase after a 30° angle of incidence, the step gets 3-5nm wider. This step could be caused by the decrease in reflective interference. Notch filters are made up of a substrate stacked with several layers of a material, whose molecular properties reflect an equal amount of light wavelengths per layer. At a 00° angle of incidence, all of the light reflected by those layers is directed back to the light’s source, and interferes with the oncoming light causing it to scatter. As the angle of incidence increases, less and less light is reflected back to the light source, thus allowing for more light to transmit.

Figure 25 illustrates the percent transmission of white light per 10° angles of incidence. Every 10° increase, the percent transmission decreases, except at a 30° angle of incidence. It is possible that at a 30° angle of incidence, the 532NF’s internal refractive properties act in such a way that more light is allowed to transmit to the spectrometer’s sensor. Also as the angle of incidence increases, the percent transmission of light in the notch portion of the spectrum increases. At a 00° angle of incidence, the percent transmission is 5%; however, at a 30° angle of incidence, the percent transmission increases to 8%, and an additional 2-3% every 10° angle of incidence increase. This suggests that not only does the 532NF become less effective in reflecting the light it was designed to do, it is also performing at a lower optical density.

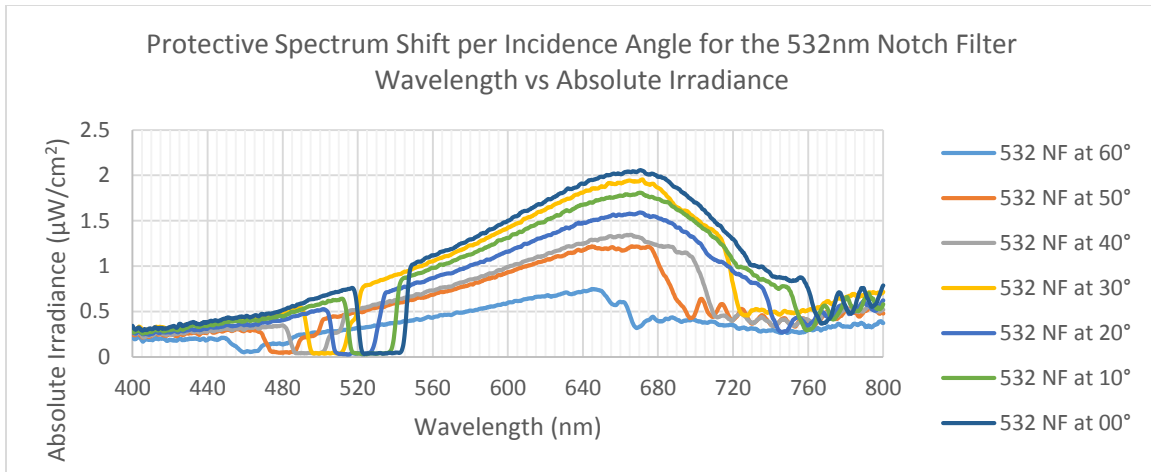


Figure 24: absolute irradiance spectrum shift per incidence angle for the 532nm notch filter

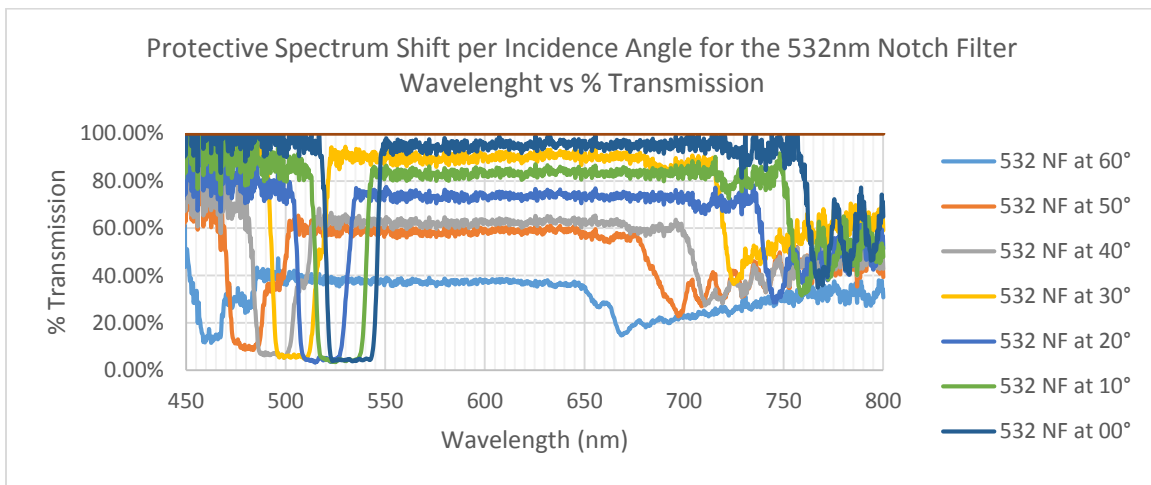


Figure 25: % transmission spectrum shift per incidence angle for the 532nm notch filter

2. Glare Production

A. Glare production photographs

Figures 26-31 are some of the pictures used to measure glare production for this study. Figure 26 had no light source, and was used as a blank to determine the color threshold for the color histograms per test sample per angle of incidence. The photographic software (ImageJ), calculated that there were no green pixels above a green intensity level of 17; therefore, any pixel measured brighter than an intensity level of 17 was counted towards the following cumulative percentile graphs. Figure 32 is an example of one of the color histograms produced by the photographic software; the other color histograms produced are located in Appendix E. For glare production measurements, green color histograms were produced because that was the color of the laser light, and the number of green pixels per intensity level was quantified. Unfortunately, 532NF’s data line gets obscured by the other data lines within these histograms, such as in Figure 32. To determine the change in glare production between the 532NF and

the uncoated test samples, the color histograms were then transformed into cumulative percentile graphs, as described in the “Methods” section. All test sample pictures were also transformed into grayscale by the photographic software to measure any reduction in overall brightness, or luminous intensity, between the 532NF and the uncoated test samples.



Figure 26: No laser, glare production

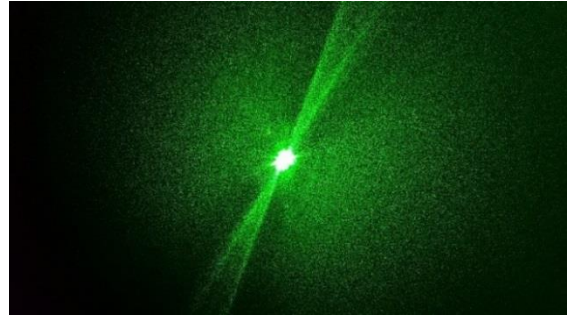


Figure 27: Laser, no test sample, glare production

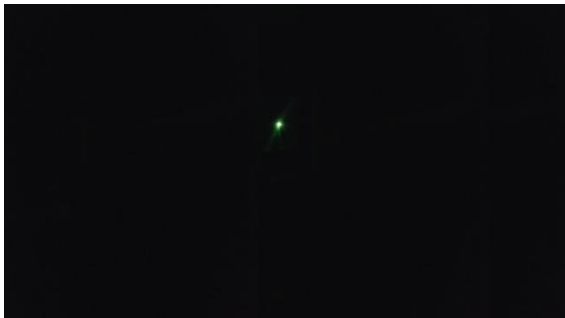


Figure 28: 532nm notch filter glare production at 00°



Figure 29: 532nm notch filter glare production at 60°

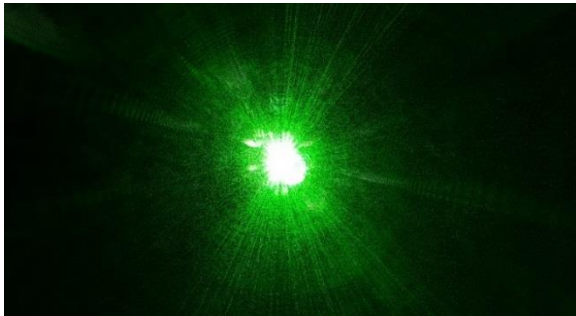


Figure 30: Test sample 2 glare production at 00°

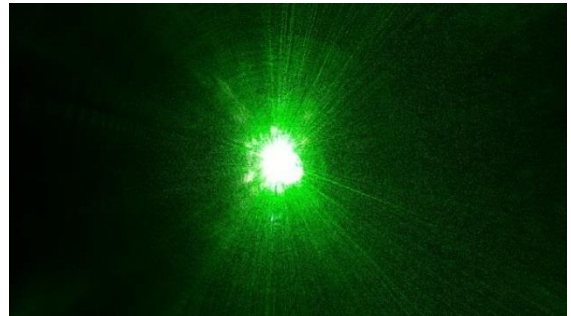


Figure 31: Test sample 2 glare production at 60°

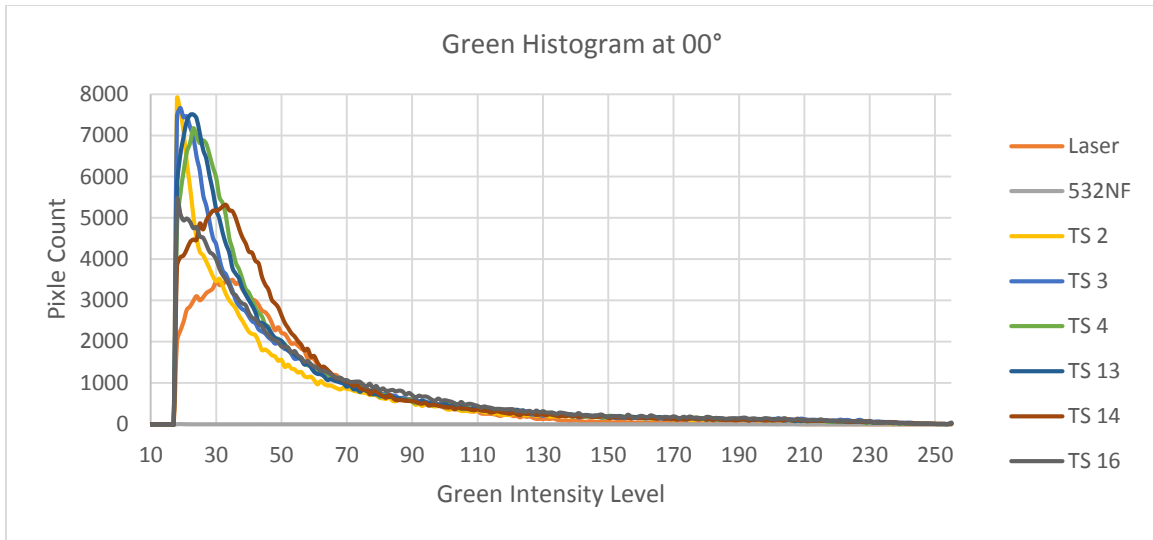


Figure 32: the green intensity of light per test sample at 00°

B. Green Histograms

i. Green histogram at 00°

All of the color histogram data provided by the photographic software for the uncoated test samples were averaged (Ave TS) and compared to the color histogram data of no light source (no laser), the laser with no test sample (laser), and the 532NF. Figure 33 is the green color intensity cumulative percentile graph at a 00° angle of incidence. Again the no light source picture acted as a blank, thus no line on the graph should have any data points less than an intensity level of 18 on the x-axis. To read this graph, each level of intensity (between 18 and 255) on the x-axis had a calculated number of pixels within each picture. As each data line travels across the x-axis, the number of pixels per intensity level gets added to the previous intensity level, measuring as a cumulative percentage. Meaning that the steeper the slope, the larger the change in color intensity. Also, the quicker a data line reaches 100%, the less intense the color is in that picture. With regards to glare production, the fewer pixels there are in the lower intensity levels, the smaller the size of the glare produced.

Figure 33 indicates that the 532NF has a drastic change in color intensity, where 70% of its green pixels are between an intensity level of 18 and 20. Furthermore, the 532NF reaches 100% of its green pixels before the laser and the Ave TS account for 70% of their own green pixels. This means that at a 00° angle of incidence, the 532NF produces almost no glare and reduces the overall green intensity of the transmitted light. Meanwhile, the Ave TS data line indicates that it produces a smaller glare than the laser (Ave TS has 70% of its pixels less than the laser), but the glare produced has a higher green intensity than the laser (Ave TS's data line is below the laser's data line between intensity levels of 60 and 255).

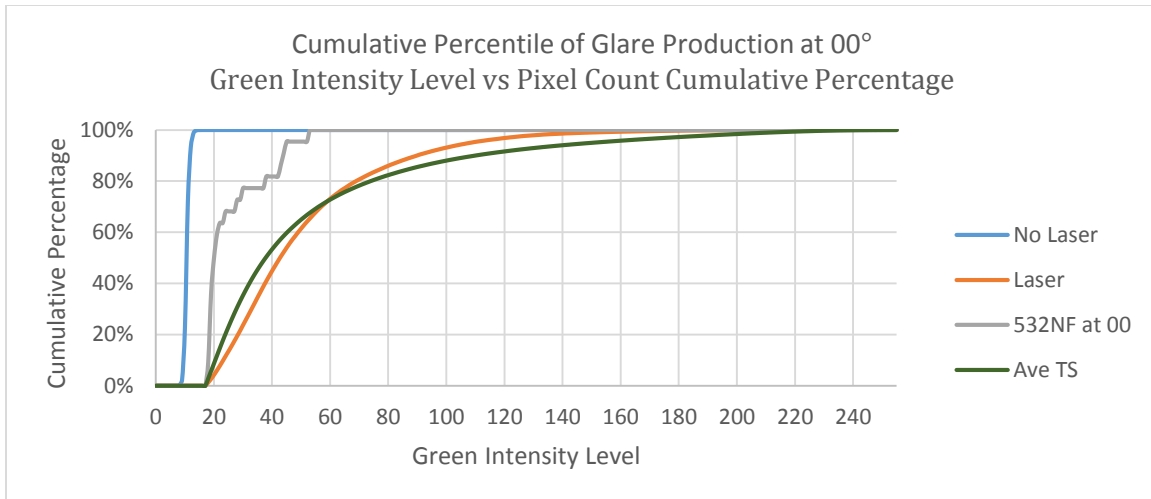


Figure 33: green intensity pixel count cumulative percentage, 532nm notch filter vs test sample average at 00°

ii. Green histogram at 60°

Figure 34 displays the pixel count cumulative percentages for the average of the uncoated test samples and the 532NF at a 60° angle of incidence. This graph shows that the 532NF and the Ave TS both produce less glare than the laser (60% of the 532NF and Ave TS pixels are less intense than the laser's), but both of their glares are more intense than the laser's (the 532NF and Ave TS take longer to reach 100% than the laser). Additionally, the transmitted light is more intense for the Ave TS than the 532NF; the graph shows the Ave TS takes much longer to reach 100%, meaning that it has many higher intensity green pixels. However, both the 532NF and the Ave TS have relatively similar sizes of glare, represented by how equal their slopes are less than an intensity level of 100.

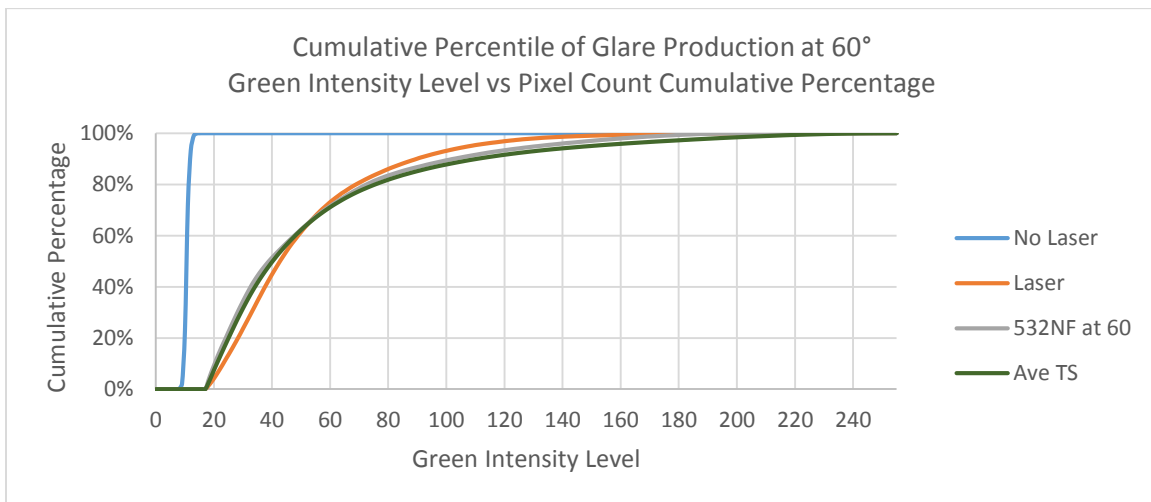


Figure 34: green intensity pixel count cumulative percentage, 532nm notch filter vs test sample average at 60°

C. Grayscale Histograms

i. Grayscale histogram at 00°

Figure 35 illustrates the cumulative percentages of the uncoated test samples, the 532NF, and the laser pictures in grayscale at a 00° angle of incidence. According to this graph, the 532NF has the smallest amount of bright pixels, because 75% of its pixels are less than an intensity level of 40, and the Ave TS has less than 65% of its pixels below an intensity level of 40 and the laser has less than 55%. However, the glare produced by the 532NF is brighter than its background when compared to the Ave TS and the laser; evident by the 532NF's data line below the others' after an intensity level of 60. This is also referred to as contrast, which is the difference between the brightest 5% of pixels and darkest 15%. The Ave TS has a smaller amount of bright pixels than the laser as well, but more than the 532NF, as seen by its data line between the other two below an intensity level of 60. The Ave TS has a larger contrast than the laser, but not as much as the 532NF's, shown by its data line between the other two above an intensity level of 60.

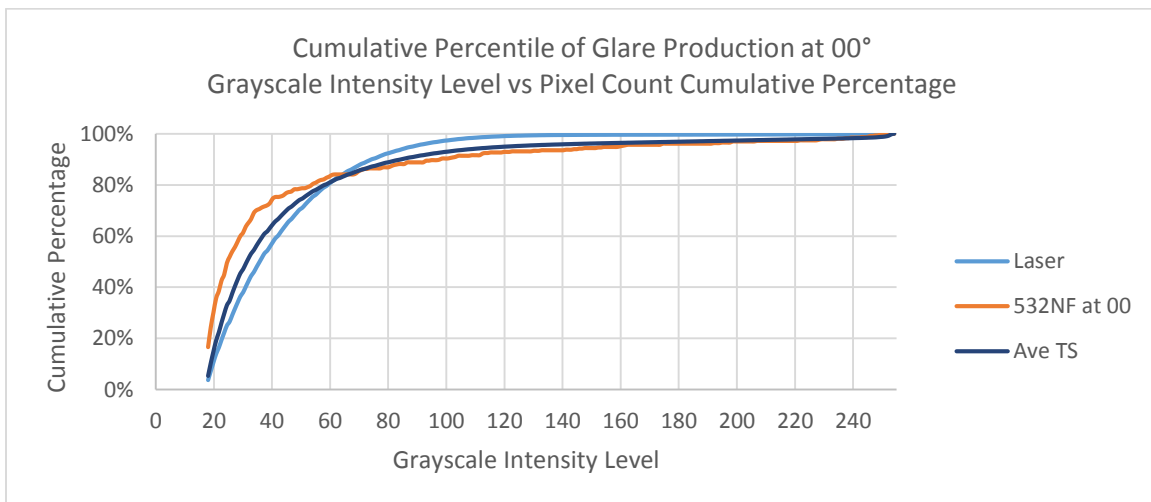


Figure 35: grayscale intensity pixel count cumulative percentage, 532nm notch filter vs test sample average at 00°

ii. Grayscale histogram at 60°

Figure 36 shows the grayscale of the test samples at a 60° angle of incidence. As before with a 00° angle of incidence, both the Ave TS and the 532NF have smaller amount of bright pixels than the laser; both have 65% of their pixels less than an intensity level of 40. Also as before, the 532NF's contrast is greater than the Ave TS's, which is greater than the laser's contrast; indicated by their data lines below the laser's after an intensity level of 80.

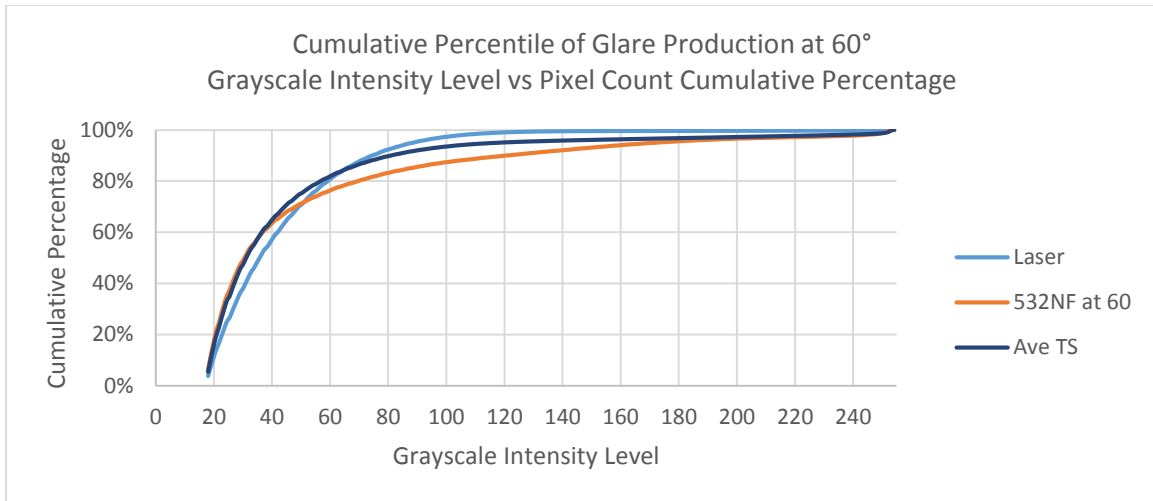


Figure 36: grayscale intensity pixel count cumulative percentage, 532nm notch filter vs test sample average at 60°

D. Cumulative percentage and contrast ratio tables

Table 1 lists the green intensity level for certain cumulative percentiles of the laser, the Ave TS, and the 532NF at a 00° angle of incidence, as well as their contrast ratios. The 532NF has a much smaller contrast ratio than the Ave TS and the laser, because its green pixels reach 100% a lot sooner than the Ave TS and the laser. This not only means that there is less glare transmitting through the 532NF, the glare transmitted has a low intensity of green light. Meanwhile, the Ave TS has less glare than the laser, because 75% of the pixels are less intense than the laser, but the glare produced is more has a higher intensity level compared to the laser, because the Ave TS contrast ratio is larger than the laser’s.

Table 2 lists the grayscale intensity level for certain cumulative percentiles of the laser, the Ave TS, and the 532NF at a 00° angle of incidence, as well as their contrast ratios. This table further suggests that the 532NF has much less glare than the Ave TS and the laser, because its’s pixels are consistently less intense. Yet, the relative brightness of the 532NF’s glare is much higher than its background when compared to the Ave TS and the laser, because the 532NF’s contrast ratio is much higher.

Table 1: Green Histogram at 00°								
Approx. Green Intensity Level per Pixel Count Cumulative Percentage								
Test Sample	0%	15%	25%	50%	75%	95%	100%	Contrast Ratio (95%/15%)
No Laser	6	9-10	10	10-11	11	12	16	unknown
Laser	17	26	31	43	62	108	226	4.15
532NF	17	18	18-19	20	30	45	53	2.50
Ave TS	17	22	26	38	64	150	255	6.82
Ave Flat	17	22	25	36	63	150	255	6.82
Ave Curved	17	23	27	39	65	150	255	6.52

Table 2: Grayscale Histogram at 00°								
Approx. Grayscale Intensity Level per Pixel Count Cumulative Percentage								
Test Sample	0%	15%	25%	50%	75%	95%	100%	Contrast Ratio (95%/15%)
Laser	<18	21	24	36	54	88	254	4.19
532NF	<18	18	19	24	41	160	250	8.87
Ave TS	<18	20	23	31	50	122	254	6.13
Ave Flat	<18	20	23	31	51	126	254	6.36
Ave Curved	<18	20	23	31	50	117	254	5.90

Table 3 lists the green intensity level for certain cumulative percentiles of the Ave TS, and 532NF at a 60° angle of incidence, as well as their contrast ratios. At this angle of incidence, the size of the glare for the 532NF and the Ave TS are about equal to each other, because their intensity levels per cumulative percentage are about the same until 95%. At 95%, the 532NF attenuates the laser’s light better than the Ave TS, because the 532NF reaches 100% quicker than the Ave TS, meaning that the 532NF produces a less intense glare.

Table 4 lists the grayscale intensity level for certain cumulative percentiles of the Ave TS, and 532NF at a 60° angle of incidence, as well as their contrast ratios. Just as seen in Figure 36, the relative size of the glares produced by the 532NF and the Ave TS are about the same; their intensity levels do not greatly differ until after 50% of the pixels are accounted for. Yet, the relative brightness of the glare for the 532NF is much greater to its background than the Ave TS, because the 532NF has a much higher intensity level when it reaches 100% and the contrast ratio is 45% larger than the Ave TS.

Table 3: Green Histogram at 60°								
Approx. Green Intensity Level per Pixel Count Cumulative Percentage								
Test Sample	0%	15%	25%	50%	75%	95%	100%	Contrast Ratio (95%/15%)
No Laser	6	9	10	10-11	11	12	16	1.33
Laser	18	26	31	43	62	108	226	4.15
532NF	18	22	26	39	65	132	214	6.00
Ave TS	18	23	27	40	66	150	255	6.52
Ave Flat	18	23	27	40	64	150	255	6.52
Ave Curved	18	23	27	40	67	150	255	6.52

Test Sample	0%	15%	25%	50%	75%	95%	100%	Contrast Ratio (95%/15%)
Laser	<18	21	24	36	54	88	254	4.25
532NF	<18	20	22	31	57	172	254	8.65
Ave TS	<18	20	23	31	49	118	254	5.94
Ave Flat	<18	20	22	30	48	118	254	5.94
Ave Curved	<18	20	23	33	52	117	254	5.90

Tables 5 and 6 display the p-values for each set of results to determine if there is a significant difference between the flat uncoated test samples and the curved uncoated samples, and between the 532NF and the uncoated test samples. The tests performed were two-tailed t-tests with unequal variances; the significance level was set at 5%. Table 5 displays the results for the flat vs curved uncoated test samples. This table indicates that there was no significant difference between the two types of test samples at any cumulative percentile within the green or grayscale pictures at a 00° or 60° angle of incidence.

Table 6 displays the results for the 532NF vs the uncoated test samples. At an 00° angle of incidence, the 532NF is significantly different than the uncoated test samples at every cumulative percentile and with the contrast ratio, which was expected. From Figure 35 and Table 2, it is clear that the 532NF’s glare is much smaller in size than the Ave TS, and is a lot less intense than the Ave TS. At a 60° angle of incidence, the green histogram data indicates that there is no significant difference between the 532NF’s and the uncoated test samples’ glare size, which is also evident by their similar slopes in Figure 6. However, the significant difference between their contrast ratios suggests that the glare produced by the uncoated test samples are more intense than the 532NF’s glare. The grayscale at a 60° angle of incidence indicates that the 532NF and the uncoated test samples are the same at 50%, but significantly different above and below 50%. This suggests that Figure46 may be incorrect in interpreting their glare sizes to be the same below 50%. Yet, the fact that the relative brightness of the 532NF’s glare is much smaller than the uncoated test samples seems correct with a calculated significant difference at the 75th percentile and with the contrast ratio.

	25%	50%	75%	Contrast Ratio
Green at 00°: p =	0.173	0.268	0.737	0.235
Grayscale at 00°: p =	0.423	0.751	0.931	0.439
Green at 60°: p =	0.567	0.765	0.381	0.933
Grayscale at 60°: p =	0.225	0.095	0.143	0.736

Table 6: p-values - 532NF vs Average TS				
	25%	50%	75%	Contrast Ratio
Green at 00°: p =	<0.0001	<0.0001	<0.0001	<0.0001
Grayscale at 00°: p =	<0.0001	<0.0001	<0.0001	<0.0001
Green at 60°: p =	0.0991	0.4931	0.4084	0.0089
Grayscale at 60°: p =	0.0327	1.000	0.0036	<0.0001

3. Color Distortion

A. Color Reference Card

Figures 37-39 are some of the pictures used to calculate the green, red, and blue histograms and their respective cumulative percentile graphs. Color reference cards (CRC) like this one are an industry standard for photographers because it has a wide range of colors and brightness levels, which is why it was chosen for this study. The CRC could act as a control between different studies to compare results. Figure 38 is with the 532NF taped over the camera’s aperture, thus the green square in the upper left of the picture is a little darker than the rest of the pictures, due to some of the green being reflected away from the camera by the 532NF. The right side of Figure 38 has a little more orange hue to it than the other pictures, also because the 532NF is reflecting away some of the green color.



Figure 37: No test sample color distortion of CRC



Figure 38: 532 notch filter color distortion of CRC



Figure 39: Test sample 2 color distortion of CRC

i. Green histogram data of the color reference card

Figure 40 is the green cumulative percentile graph for the CRC. The CRC has various levels of green intensity in it by design, thus the contrast ratio for the No TS is rather small at 3.45; the lowest and highest cumulative percentiles of intensity are fairly similar and the data lines travel along the entire x-

axis before reaching 100%. Figure 37 shows a darker green square for the 532NF than the other pictures, and Figure 40 further proves this. The 532NF has more green pixels in the lower intensity levels than the No TS or the Ave TS, after an intensity level of 110. The Ave TS and the No TS share approximately the same number of pixels per intensity level after 110. Before an intensity level of 110, it appears that the uncoated test samples scatter some of the green light, preventing it from being captured by the camera. Whereas, the 532NF and the No TS are fairly equal below an intensity level of 110. This means that the 532NF is better at reflecting more intense green light, but not so effective in reflecting less intense green light. The opposite appears to be true for the uncoated test samples.

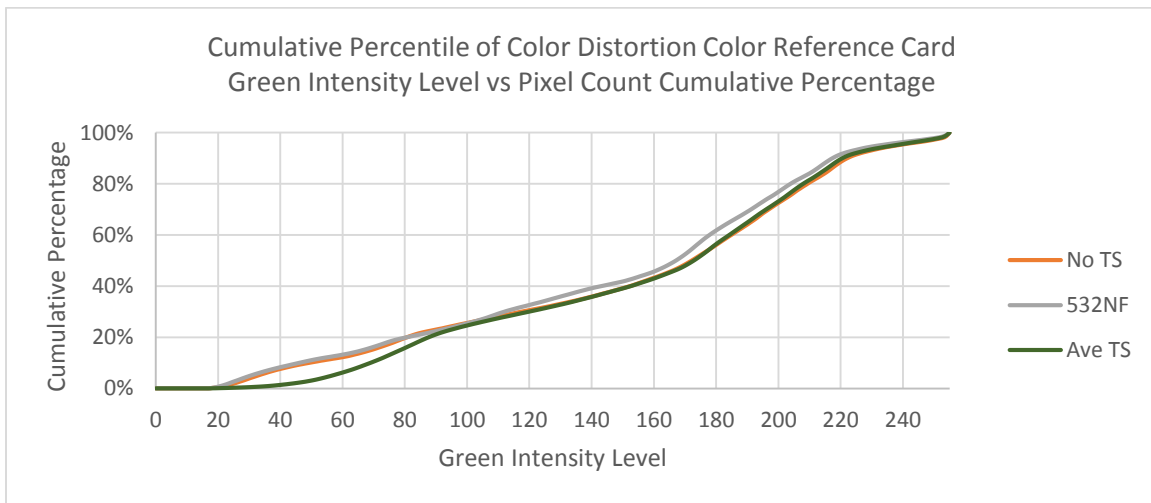


Figure 40: green intensity pixel count cumulative %, 532 notch filter vs test sample average for the color reference card

ii. Red histogram data of the color reference card

Figure 41 is the red cumulative percentile graph for the CRC. There appears to be some color shifting as the 532NF reflects more green light in the higher intensities. The 532NF is about equal with the No TS below a red intensity level of 60. As the 532NF reflects higher intensity level green light, its overall color became a little redder with an increase in red intensity; the 532NF data line suggests that it transmits more intense red pixels than the No TS until it syncs up with the Ave TS, between a red intensity level of 60 and 120. The Ave TS seems to scatter more red light away from the camera than the 532NF, because its cumulative percentage takes longer to reach the same as the 532NF as the intensity level increases. This may be due to a coating applied to the window test samples during its manufacturing, or the plexi-glass does not transmit red light as effectively as the 532NF, which is made of glass. All three data lines follow the same pattern after an intensity level of 140, possibly do to the detection of the red and pink color squares in the pictures.

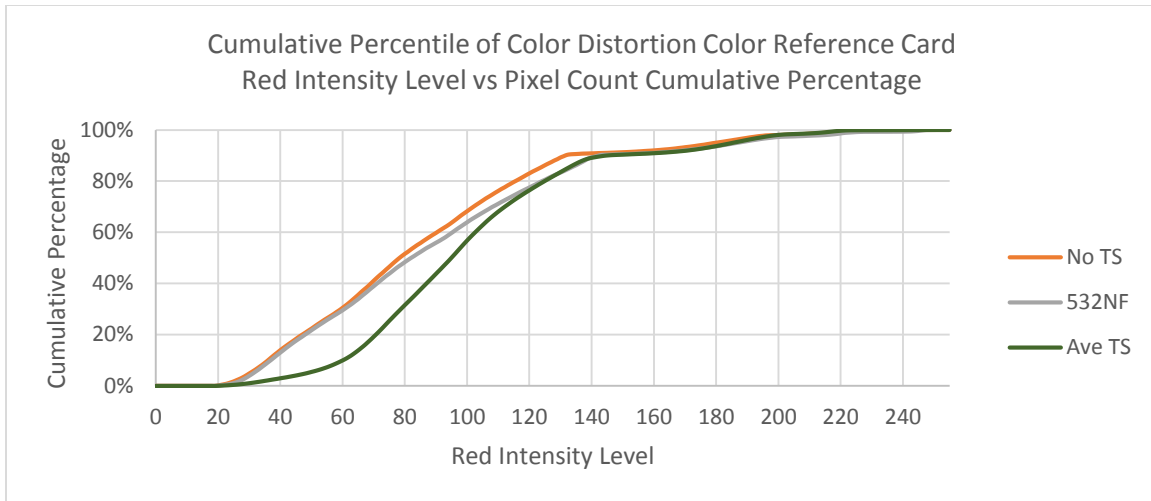


Figure 41: red intensity pixel count cumulative %, 532 notch filter vs test sample average for the color reference card

iii. Blue histogram data of the color reference card

Figure 42 is the blue cumulative percentile graph for the CRC. There does again appear to be a color shifting by the 532NF, but this time the 532NF is attenuating blue light between intensity levels of 30 and 120. The Ave TS seems to scatter more blue light away from the camera than the 532NF between intensity levels of 20 and 50, evident by the rounded shape of its data line. This may be due to a coating applied to the window test samples during its manufacturing, or the plexi-glass may not transmit blue light as effectively as the 532NF due to its internal absorptive properties. All three data lines follow the same pattern after an intensity level of 130, possibly due to the detection of the dark blue square, and steps up at an intensity level of 160 due to the bright blue square.

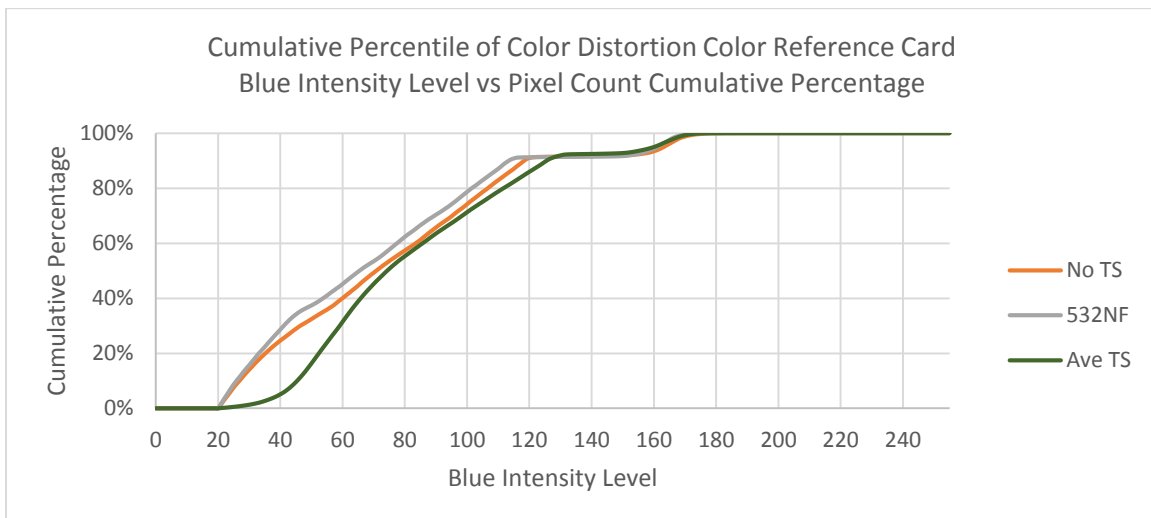


Figure 42: blue intensity pixel count cumulative %, 532 notch filter vs test sample average for the color reference card

iv. Cumulative percentage and contrast ratio tables the color reference card

Table 7: Green Histogram at 00°								
Approx. Green Intensity Level per Pixel Count Cumulative Percentage								
Test Sample	0%	15%	25%	50%	75%	95%	100%	Contrast Ratio (95%/15%)
No Laser	6	9-10	10	10-11	11	12	16	
No TS	17	69	98	172	203	238	255	3.45
532NF	17	67	99	167	198	232	255	3.46
Ave TS	17	79	101	173	202	237	255	3.00

Table 8: Red Histogram at 00°								
Approx. Red Intensity Level per Pixel Count Cumulative Percentage								
Test Sample	0%	15%	25%	50%	75%	95%	100%	Contrast Ratio (95%/15%)
No Laser	6	9-10	10	10-11	11	12	17	
No TS	19	41	53	78	109	180	230	4.39
532NF	19	42	54	82	116	187	250	4.45
Ave TS	19	66	75	95	118	185	251	2.80

Table 9: Blue Histogram at 00°								
Approx. Blue Intensity Level per Pixel Count Cumulative Percentage								
Test Sample	0%	15%	25%	50%	75%	95%	100%	Contrast Ratio (95%/15%)
No Laser	8	11-12	12	12-13	13	14	18	
No TS	18	31	40	71	101	163	190	5.26
532NF	18	29	37	65	96	161	187	5.55
Ave TS	18	49	56	74	105	160	183	3.27

Tables 7-9 displays the color intensities of certain cumulative percentages for the 532NF picture, the average of the uncoated test samples' pictures, and the picture with no test sample for the CRC. As stated previously, the green histogram provided a much smaller contrast ratio because of the more various levels of green intensities than the red or the blue. The Ave TS consistently had smaller contrast ratios than the 532NF and No TS for all three colors, possibly due to the uncoated test samples being unable to transmit the lower intensity levels of each color. The 532NF's green contrast ratio is almost equal to the No TS's; the 532NF seems to be more efficient in reflecting higher intensity level green light, but the CRC does not have a large concentration of green color in it. The 532NF did cause a red spectrum shift; possibly because as the 532NF reflects away some green light its picture takes on a slight orange hue, because the color shifted into the red spectrum. However, increase in red intensity was not

very large, so the 532NF contrast ratio was only slightly above the No TS's. Additionally, the 532NF has a higher contrast ratio for the blue histogram compared to the No TS as well. The blue light intensity is not greatly attenuated by the 532NF, so its contrast ratio is again only slightly above the No TS's. Due to the increase in red intensity and decrease in blue intensity by the 532NF, Figure 38 appears to be somewhat more yellow or tan than the other test sample pictures of the CRC.

B. Scenario 1

Figures 43-46 are some of the pictures of scenario 1 used to calculate the green, red, and blue histograms and their respective cumulative percentile graphs. This scene was used because it is at night, with a red flare in the background and a vague horizon. A very important event that pilots wouldn't want to miss because of the thin film coating. This scenario does not have much color variability and is not very bright. The idea was to show that the 532NF doesn't hamper the pilot's ability to see the flare or horizon. Just by looking at Figure 44, there does not appear to be much of a difference between the 532NF picture and the other pictures.



Figure 43: No test sample color distortion of scenario 1



Figure 44: 532 notch filter color distortion of scenario 1



Figure 45: Test sample 2 color distortion of scenario 1

i. Green histogram data of scenario 1

Figure 46 is the green cumulative percentile graph for scenario 1. Since there is some green in the scenario, the 532NF does reflect some of the green light away from the camera, evident by its data line diverging from the other two between intensity levels of 60-100. Yet since there is not a large amount of intense green light, the divergence is barely registerable. This means that the 532NF may be better at reflecting the higher intensity level green light than the lower intense green light; it reflected very little

green light in scenario 1 compared to the CRC, which had a lot more intense green light in it. The Ave TS, though, does not reflect or scatter green light in this scenario.

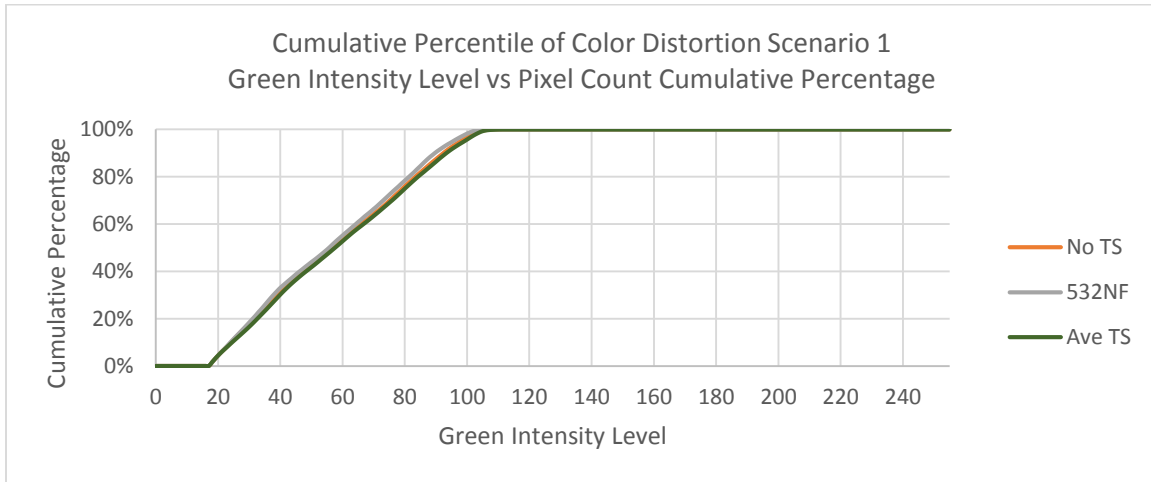


Figure 46: green intensity pixel count cumulative %, 532 notch filter vs test sample average for scenario 1

ii. Red histogram data of scenario 1

Figure 47 is the red cumulative percentile graph for scenario 1. Like the green histogram data, scenario 1's data lines quickly reach 100% for the red histogram, but the red intensity levels are fairly uniform, thus the contrast ratio for the No TS is small (3.48 for the 95%/15%) compared to the CRC. The 532NF does not produce a red spectrum shift within the scenario possibly due to the lack of higher intense green light. Since the green intensity level in this scenario is low compared to the CRC, the 532NF does not reflect as much of the green light away from the camera, evident by its data line equaling the other two. The CRC had more intense green light within its pictures; therefore, the 532NF reflected a lot of green light away shifting the picture into the red spectrum. Since scenario 1 had less pixels in the higher green intensity levels, less of its picture was shifted into the red.

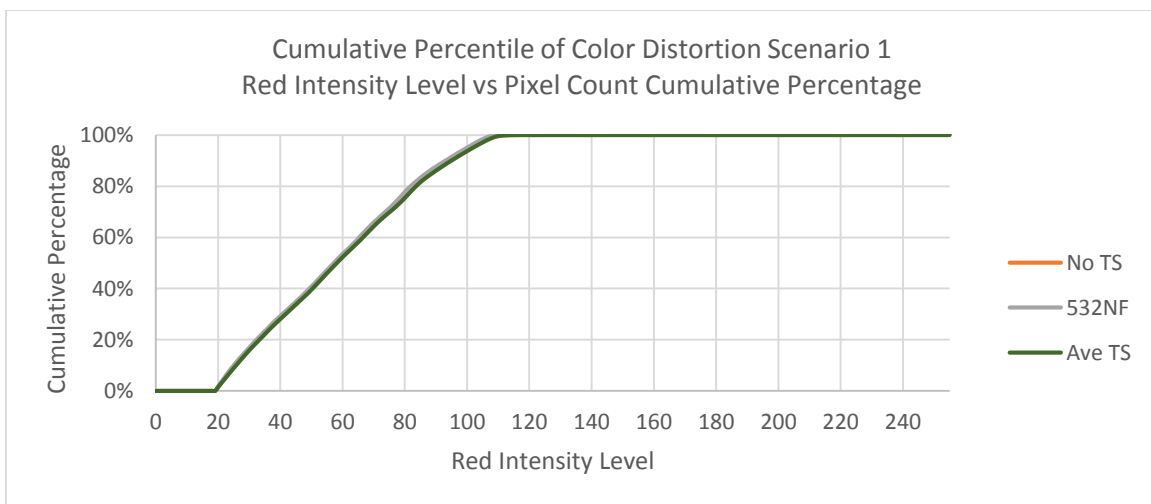


Figure 47: red intensity pixel count cumulative %, 532 notch filter vs test sample average for scenario 1

iii. Blue histogram data of scenario 1

Figure 48 is the blue cumulative percentile graph for scenario 1. Since there is little higher intensity green light in the scenario, the 532NF does not attenuate as much of the blue light away from the camera as it did with the CRC, evident by its data line diverging from the other two after an intensity level of 60. There is some green light within this scenario reflected away the camera by the 532NF just like the CRC; therefore, the 532NF decreased the intensity of blue light between the cumulative percentiles of 40%-98%, even though scenario 1 did not experience an increase in red light intensity.

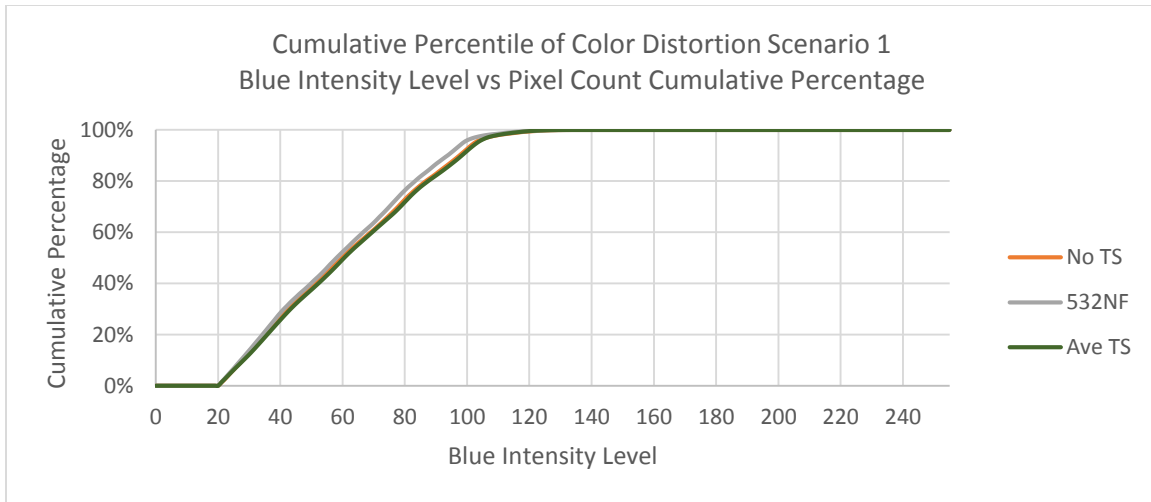


Figure 48: blue intensity pixel count cumulative %, 532 notch filter vs test sample average for scenario 1

iv. Cumulative percentage and contrast ratio tables for scenario 1

Table 10: Green Histogram								
Approx. Green Intensity Level per Pixel Count Cumulative Percentage								
Test Sample	0%	15%	25%	50%	75%	95%	100%	Contrast Ratio (95%/15%)
No Laser	6	9-10	10	10-11	11	12	16	
No TS	17	28	35	57	79	98	111	3.50
532NF	17	28	34	56	77	95	108	3.39
Ave TS	17	29	36	58	80	99	112	3.41

Table 11: Red Histogram								
Approx. Red Intensity Level per Pixel Count Cumulative Percentage								
Test Sample	0%	15%	25%	50%	75%	95%	100%	Contrast Ratio (95%/15%)
No Laser	6	9-10	10	10-11	11	12	17	
No TS	19	29	36	58	79	101	118	3.48
532NF	19	29	36	57	78	100	116	3.45
Ave TS	19	29	37	58	80	102	117	3.52

Table 12: Blue Histogram								
Approx. Blue Intensity Level per Pixel Count Cumulative Percentage								
Test Sample	0%	15%	25%	50%	75%	95%	100%	Contrast Ratio (95%/15%)
No Laser	8	11-12	12	12-13	13	14	18	
No TS	20	32	39	60	82	103	134	3.22
532NF	20	31	38	58	79	99	133	3.19
Ave TS	20	32	39	61	83	103	132	3.22

Tables 10-12 display the color intensities of certain cumulative percentages for the 532NF, the uncoated test sample average, and the no test sample of scenario 1. For this scenario, all three colors reached 100% much quicker than the CRC; however, since each color’s intensities were fairly uniform throughout the histograms, the contrast ratios were more consistent than they were for the CRC. Although the contrast ratios were consistently similar per color, the cumulative percentiles show some divergence by the 532NF in the green and blue histograms. The 532NF seems to be more effective in reflecting higher intensity green light because it only diverges away between 75%-95%. The data suggests that the increase in red intensity only happen when there is higher intensity green light; there is an apparent increase in red intensity in the CRC histograms, but not in the scenario 1 histograms. Also, the blue light intensity seems to be decreased if any green light is reflected, because the blue light is reflected away from the camera for both the CRC histograms and the scenario 1 histograms.

C. Scenario 2

Figures 49-51 are some of the pictures of scenario 2. This scene was used because it is another common event that pilots wouldn’t want to miss out on because of color distortion. Again, there isn’t much color variation like in scenario 1, but this scenario is brighter and has a clear indication of where the horizon is. You can also clearly see the orange jacket on the vessel pilot, even with the 532NF. Figure 50 is with the 532NF taped over the camera’s aperture, and appears to have a darker image when compared to the other pictures.



Figure 49: No test sample color distortion of scenario 2



Figure 50: 532 notch filter color distortion of scenario 2



Figure 51: Test sample 2 color distortion of scenario 2

i. Green histogram data of scenario 2

Figure 52 is the green cumulative percentile graph for scenario 2. The green light in this scenario is more intense than in scenario 1, so the 532NF reflects more of the green light away. This is evident by the 532NF data line diverging from the other two at an intensity level 18 and with a larger gap between them than in scenario 1. Since the 532NF is better at reflecting the higher intensity level green light, its data line diverges more and more away as the intensity level increases until the 532NF reaches approximately 98% of its cumulative percentage. The Ave TS, though, does not reflect or scatter green light in this scenario; therefore, its green contrast ratio is very similar to the No TS.

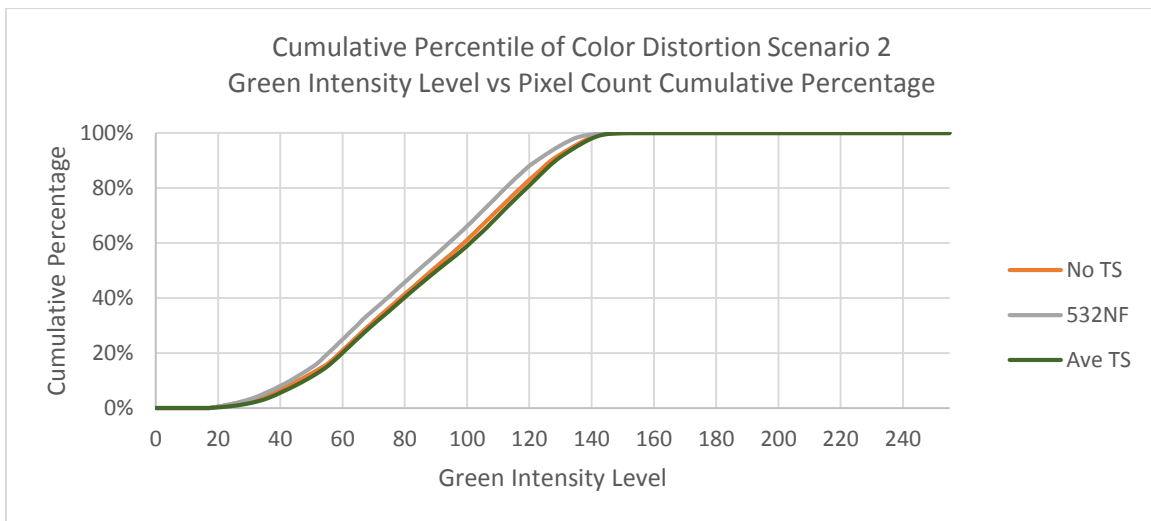


Figure 52: green intensity pixel count cumulative %, 532 notch filter vs test sample average for scenario 2

ii. Red histogram data of scenario 2

Figure 53 is the red cumulative percentile graph for scenario 2. Since there is little high intensity green light in the scenario compared to the CRC, the 532NF does not increase the intensity of the red light by reflecting away the green. Since the CRC had a lot of intense green light, there occurred a red spectrum shift, but like scenario 1, scenario 2 does not have as much intense green light, thus no increase in the intensity of the red light occurs.

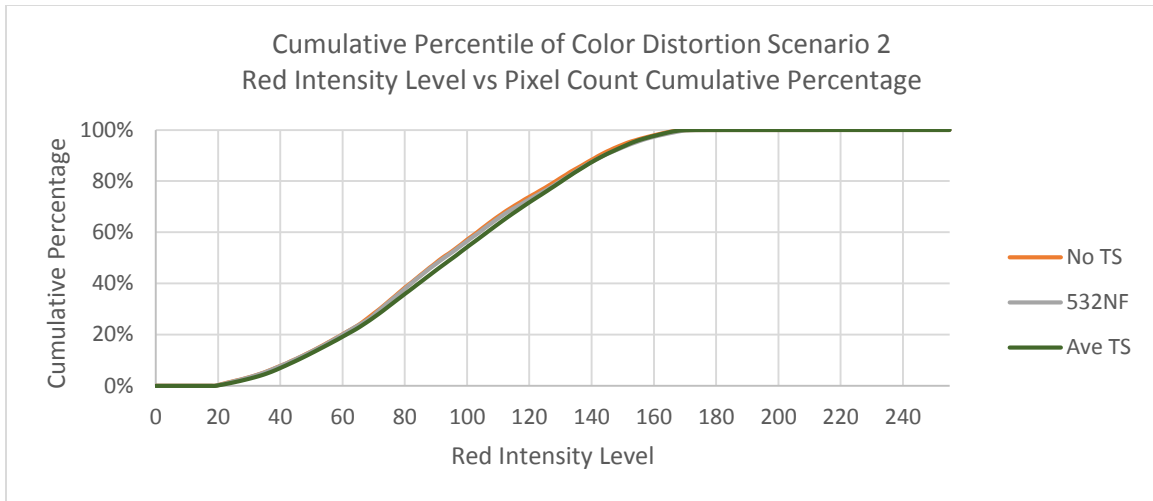


Figure 53: red intensity pixel count cumulative %, 532 notch filter vs test sample average for scenario 2

iii. Blue histogram data of scenario 2

Figure 54 is the blue cumulative percentile graph for scenario 2. Since there is some intense green light in the scenario, the 532NF does reflect a lot more of the blue light away from the camera than it did in scenario 1, evident by its data line diverging after an intensity level of 18. Even though scenario 2 did not experience much change in the red intensity levels, the 532NF's notched spectrum was able to manipulate the blue light just like in the CRC and scenario 1 pictures. Since the 532NF was able to reflect green light away for 98% of its cumulative percentage, it attenuated blue light for approximately 98% of its cumulative percentage compared to the Ave TS and the No TS. This may explain why Figure 50 appears a little darker than the other scenario 2 pictures.

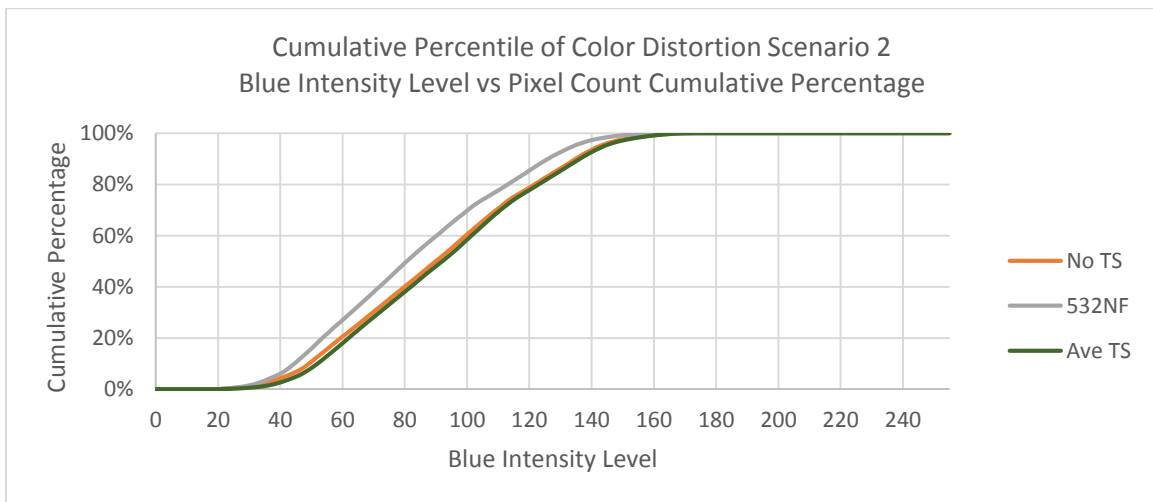


Figure 54: blue intensity pixel count cumulative %, 532 notch filter vs test sample average for scenario 2

iv. Cumulative percentage and contrast ratio tables for scenario 2

Table 13: Green Histogram								
Approx. Green Intensity Level per Pixel Count Cumulative Percentage								
Test Sample	0%	15%	25%	50%	75%	95%	100%	Contrast Ratio (95%/15%)
No Laser	6	9-10	10	10-11	11	12	16	
No TS	17	54	64	89	113	134	152	2.48
532NF	17	50	60	84	108	129	150	2.58
Ave TS	17	55	65	90	115	135	153	2.45

Table 14: Red Histogram								
Approx. Red Intensity Level per Pixel Count Cumulative Percentage								
Test Sample	0%	15%	25%	50%	75%	95%	100%	Contrast Ratio (95%/15%)
No Laser	6	9-10	10	10-11	11	12	17	
No TS	19	52	67	92	122	152	219	2.92
532NF	19	53	67	93	123	154	215	2.91
Ave TS	19	54	68	95	124	153	214	2.83

Table 15: Blue Histogram								
Approx. Blue Intensity Level per Pixel Count Cumulative Percentage								
Test Sample	0%	15%	25%	50%	75%	95%	100%	Contrast Ratio (95%/15%)
No Laser	8	11-12	12	12-13	13	14	18	
No TS	20	54	65	90	115	143	177	2.65
532NF	20	49	58	81	106	134	169	2.73
Ave TS	20	57	67	92	116	144	174	2.53

Tables 13-15 display the color intensities of certain cumulative percentages for the 532NF picture, the average of the uncoated test samples' pictures, and the picture with no test sample for scenario 2. For scenario 2, all three colors took a little longer to reach the 100% cumulative percentile than scenario 1, and because each color's intensities were fairly uniform throughout the histograms, the contrast ratios were more consistent between the colors, but less than those for scenario 1. Both the contrast ratios and the cumulative percentiles showed some divergence by the 532NF in the green and blue histograms when compared to the Ave TS and the No TS, but not within the red histogram. Since the 532NF reflected some green light away from the camera in Figure 52, it also attenuated some blue light as seen in Figure 54. Additionally, just like scenario 1, there is a lack of higher intensity levels of green light (such as in the CRC pictures), so there is no change to the red histogram in scenario 2 by the 532NF.

D. Scenario 3

Figures 55-57 are some of the pictures of scenario 3. This scene was chosen because most thin film coatings tend to take on a red or orange hue when absorbing/reflecting green light, and it was desired to see if the 532NF would distort the orange smoke flare. Pilots would not want to miss the orange smoke flare because they could not see it due to the thin film coating. Figure 56 is the 532NF of scenario 3, and there does appear to be a pinkish hue to it when compared to the other pictures; however, the orange smoke flare and the lifejacket can still clearly be seen, and only the water takes on the pink hue.



Figure 55: No test sample color distortion of scenario 3



Figure 56: 532 notch filter color distortion of scenario 3



Figure 57: Test sample 2 color distortion of scenario 3

i. Green histogram data of scenario 3

Figure 58 is the green cumulative percentile graph for scenario 3. This scenario's image has more green pixels in the higher intensity levels than scenarios 1 and 2, because its contrast ratio is larger for the green than scenarios 1 and 2. Consequently, the 532NF reduces the intensity level of the green light more than scenarios 1 and 2; this is evident by the 532NF data line diverging from the other two at an intensity level 20 and with a larger gap between them than in scenario 1 or 2. Since the 532NF is better at reflecting the higher intensity level green light, its data line diverges more and more away as the intensity level increases until the 532NF reaches approximately 98% of its cumulative percentage. The Ave TS, though, does not reflect or scatter green light in this scenario; therefore, its green contrast ratio is very similar to the No TS.

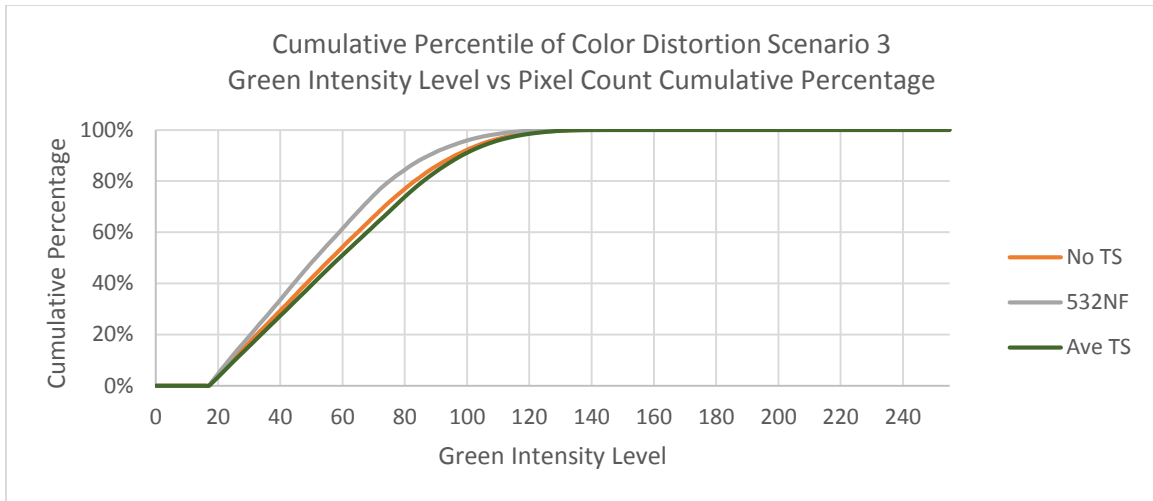


Figure 58: green intensity pixel count cumulative %, 532 notch filter vs test sample average for scenario 3

ii. Red histogram data of scenario 3

Figure 59 is the red cumulative percentile graph for scenario 3. Scenario 3 has a lot of red light within it due to the orange smoke flare; therefore, the data lines do not reach 100% until a red intensity level of 255. As such, the contrast ratio for the No TS is larger than any other scenario’s red histogram. Due to the larger number of green pixels in the higher intensity levels and the larger contrast ratio for the red histogram, the 532NF noticeably increases the intensity of red light as it reflects green light; the 532NF’s data line consistently has more red pixels in the higher intensity levels over the entire graph. This is why scenario 3 takes on a pinkish hue, but scenarios 1 and 2 do not for the 532NF.

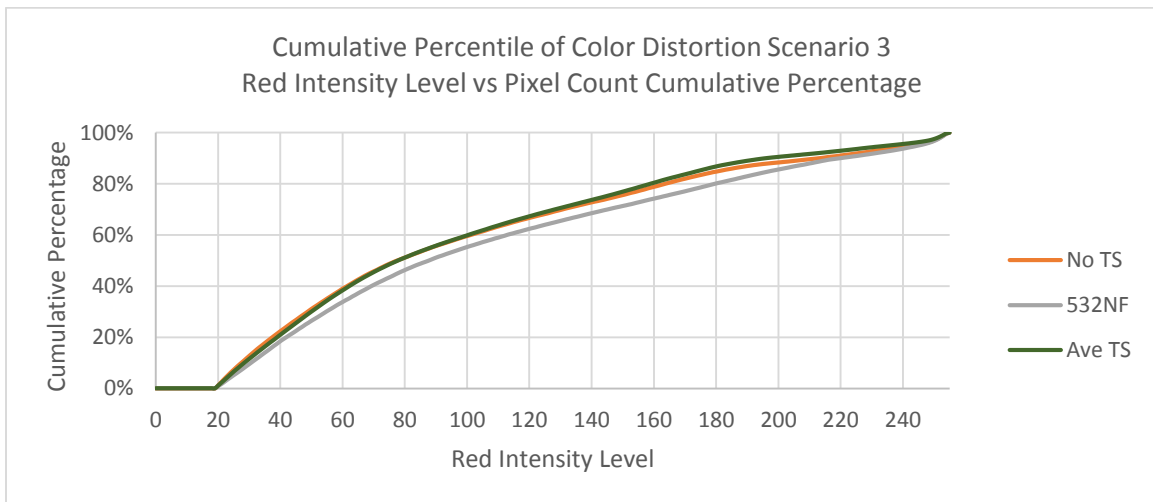


Figure 59: red intensity pixel count cumulative %, 532 notch filter vs test sample average for scenario 3

iii. Blue histogram data of scenario 3

Figure 60 is the blue cumulative percentile graph for scenario 3. Like the red histogram data, Scenario 3’s data lines take longer to reach 100% for the blue histogram, and the blue intensity levels is not very uniform throughout the graph. This leads to the contrast ratio for the No TS being larger than the other

two scenarios. Since there is some intense green light in the scenario, the 532NF does decrease the intensity of the blue light more than it did in scenario 1 and 2, evident by its data line diverging between an intensity level of 20 and 160.

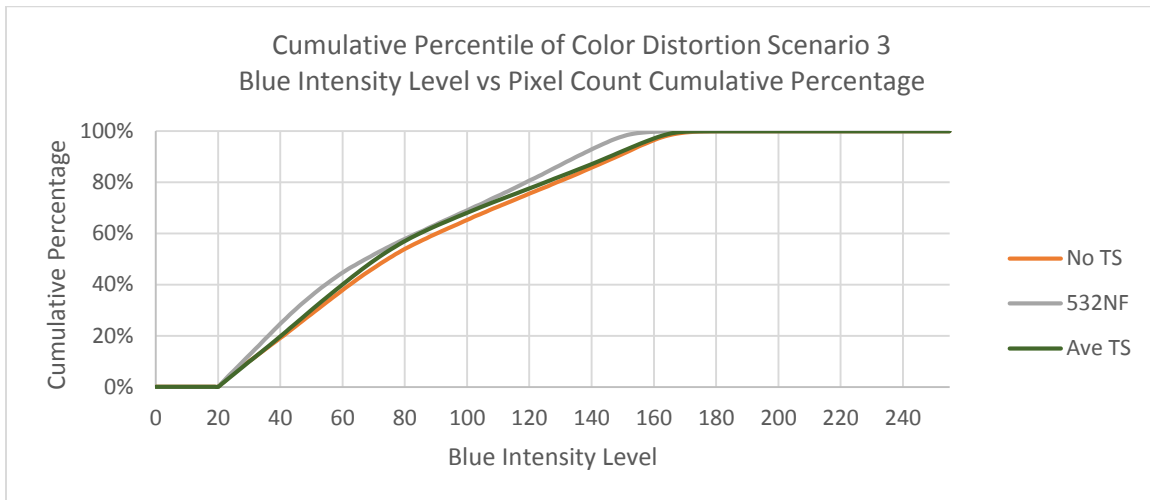


Figure 60: blue intensity pixel count cumulative %, 532 notch filter vs test sample average for scenario 3

iv. Cumulative percentage and contrast ratio tables for scenario 3

Tables 16-18 display the color intensities of certain cumulative percentages for the 532NF picture, the average of the uncoated test samples’ pictures, and the picture with no test sample for scenario 3. For scenario 3, both the contrast ratios and the cumulative percentiles showed some divergence by the 532NF in the green, red, and blue histograms when compared to the Ave TS and the No TS. There seemed to more green pixels of higher intensity in this scenario than scenarios 1 or 2; therefore, more green light was reflected. Since the 532NF reflected some green light away from the camera in Figure 58, it also attenuated some blue light as seen in Figure 60.

Table 16: Green Histogram								
Approx. Green Intensity Level per Pixel Count Cumulative Percentage								
Test Sample	0%	15%	25%	50%	75%	95%	100%	Contrast Ratio (95%/15%)
No Laser	6	9-10	10	10-11	11	12	16	
No TS	17	28	36	56	78	106	144	3.79
532NF	17	27	34	51	70	98	132	3.63
Ave TS	17	30	38	59	81	108	144	3.60

Table 17: Red Histogram								
Approx. Red Intensity Level per Pixel Count Cumulative Percentage								
Test Sample	0%	15%	25%	50%	75%	95%	100%	Contrast Ratio (95%/15%)
No Laser	6	9-10	10	10-11	11	12	17	
No TS	19	32	43	77	148	243	255	7.59
532NF	19	36	48	88	163	245	255	6.81
Ave TS	19	34	44	78	144	236	255	6.94

Table 18: Blue Histogram								
Approx. Blue Intensity Level per Pixel Count Cumulative Percentage								
Test Sample	0%	15%	25%	50%	75%	95%	100%	Contrast Ratio (95%/15%)
No Laser	8	11-12	12	12-13	13	14	18	
No TS	20	36	46	75	119	157	181	4.36
532NF	20	32	40	68	110	144	168	4.50
Ave TS	20	35	45	71	114	155	178	4.43

V. DISCUSSION/CONCLUSION

To determine if the thin film coating applied to the 532NF is a viable engineering control to protect aircraft crewmembers from laser strikes, requires a discussion of how the eye perceives color and luminous intensity. The eye has two types of cells which can detect light: the rod cells detect luminous intensity in shades of gray; the cone cells detect different light wavelengths. The cone cells come in three types: S cones detect short wavelengths or “blue color,” M cones detect medium wavelengths or “green color,” and L cones detect long wavelengths or “red color” (Thewlis 2014). Figure 91 illustrates the relative sensitivity of the rod and cone cells per electromagnetic wavelength within the visual spectrum (University of New Mexico). The approximate peaks for each type of cell are 500nm for the rods, 420nm for the blue cones, 530nm for the green cones, and 560nm for the red cones.

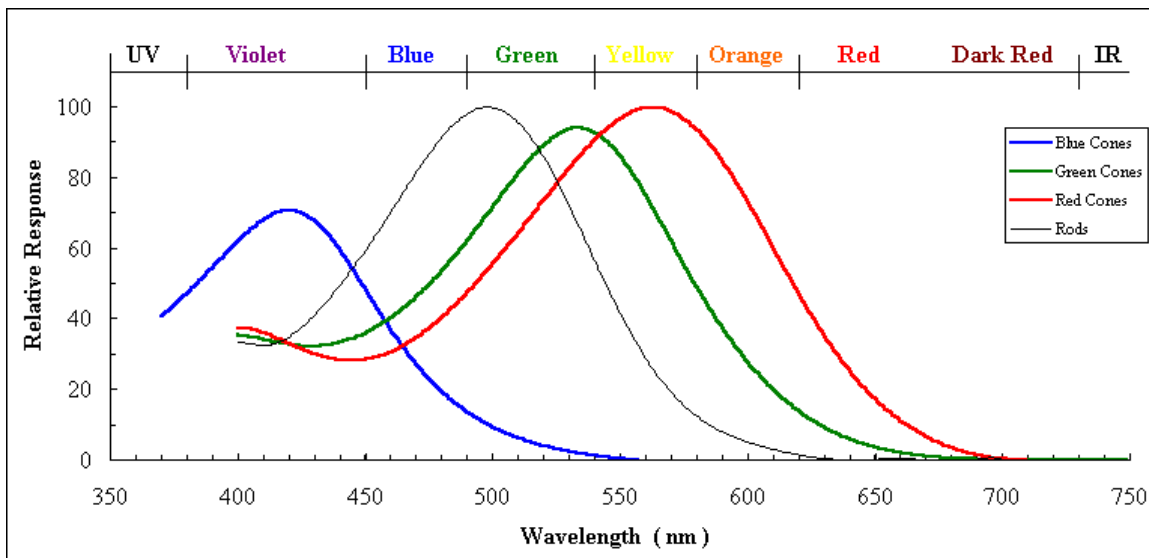


Figure 61: human eye cone visual spectrum sensitivities

Rods detect only the count of photons measuring the luminous intensity of light in shades of gray, thus allowing rods to be very effective in low light situations. Rods are located within the retina, but outside of the macula. Therefore, rods are only susceptible to the glare produced by a laser because of their luminous sensitivity, and not as much to the radiant power of the laser because of their location. Each type of cone cell detects a range of wavelengths, with a peak sensitivity according to Figure 91. Cones are solely located at very center of the macula in an area called the fovea. As seen in Figure 5, the eye focuses a laser’s light onto the fovea; therefore, the cone cells could be damaged depending on the duration of the exposure, the wavelength of the laser, and the radiant power of the laser. ANSI has set their maximum permissible exposure (MPE) limits to reflect these three factors in determining safe laser exposures to the human eye.

This study chose 532nm as the wavelength for the laser light source, because as stated in the “Background” section, the FAA data released in 2014 indicated that over 93% of reported laser strikes had a green laser beam (FAA 2015). The most common green handheld laser wavelength on the market is set at 532nm, and happens to be just about the wavelength green cone cells are most sensitive to. Taking this into account, the ANSI Z136.1-2014 MPE for 532nm is dependent on the duration of exposure. Assuming that a crewmember would blink immediately upon being struck and not try to focus their vision onto the laser beam, the exposure duration is estimated at 0.25s (the blink response time according to ANSI) (ANSI 2014). Calculated previously under the “Results” section, the MPE for a 532nm laser with a blink response is $6.36 \times 10^{-4} \text{ J} \cdot \text{cm}^2$. After multiplying the MPE by the worst case scenario, pupil dilation surface area of 8.0mm, the maximum allowable radiant power to strike a person’s eye would be 5.064mW. Although the FDA limited the sale of handheld laser pointers to <5mW in 2010, higher power laser pointers had been sold previously and are still readily available on the internet. Also, lasers can be misclassified as ANSI Class 3R but are in fact much more dangerous, as in the case with the ferry captain (Bush 2015).

To protect the cone cells from radiant power, as well as both rods and cones from luminous intensity, a thin film coating specifically designed to exclude 532nm light from transmitting was needed. However, USCG aircraft crewmembers require the ability to clearly see their surroundings to conduct flight operations, such as search and rescue, drug and migrant interdiction, and law enforcement. Hence, the thin film coating must allow as much of the visual spectrum to transmit as possible, while excluding 532nm. This type of thin film coating is referred to as a notch filter; it produces a “notch” in the visual spectrum where it excludes a range of wavelengths. Thin film coating notch filters can be designed to absorb/reflect any percentage of 532nm light by a measurement called optical density (OD); a \log_{10} scale measurement of percent transmission with 0.0 allowing 100% of light to transmit and 10.0 allowing practically no light to transmit. Since crewmembers need to clearly see their surroundings, the thin film coating must not have an OD that is too high. An OD of 4.0 was deemed appropriate because it only allows 0.01% of light to transmit, or 5mW of radiant power to transmit for a 500mW laser. 500mW is the maximum level of an ANSI Class 3B laser, and it was assumed that any laser above Class 3B would rarely be involved in an aircraft laser strike due to their difficulty to transport and their much stricter sales regulations. The 532nm laser for this study was set to a power of 90mW to represent a laser that could present a hazardous condition in the aircraft, but be low powered enough that a member of the public could easily procure it.

An engineering control would be the most practical and beneficial type of control for the crewmembers for several reasons. With the hierarchy of controls in mind, the threat of a laser strike will never be fully eliminated because it would be almost impossible for lasers to be banned from sale to the public. If lasers were banned from sale, people would still be able to get them illegally, plus all of the lasers that have already been sold would still be available to strike aircraft. The next type of control is substitution; however, the reasons against this control are the same as the ones against the elimination control. It would also be very unlikely that air travel would be substituted by other means of transportation, and even those means of travel could still be struck by lasers. Also, no technology exists that could substitute in for all of the uses that laser have.

Administrative controls have been put into place since 2004 by the FDA, FAA, FBI, and other agencies and organizations. These include fines, jail time, sales restrictions, stricter standards and regulations on the use of lasers, easier reporting methods, and better training for crewmembers on how to respond to a laser strike. Even with the increase in administrative controls, the number of laser strikes continues to almost double every year, according to the data released by the FAA (FAA 2015). There is some personal protective equipment (PPE) on the market to protect crewmembers against laser strikes. Mirror glasses, laser safety glasses, helmet visors, and night-vision goggles protect well against laser light, but as PPE, they should be the last form of control used. PPE depends on the employer supplying the crewmember, the crewmember being trained on the PPE's proper use, the crewmember actually wearing and maintaining the PPE, and PPE is generally mass produced and may not provide enough protection from the specific exposure.

An engineering control can be applied to the aircraft during manufacturing, and the crewmember can then conduct their operations without worrying about the hazards of laser strikes. Applying the thin film coating to the aircraft window seemed the most appropriate form of engineering control. Replacing the windows with cameras was not an attractive alternative to USCG pilots or USCG headquarters, due to total reliance on the cameras never malfunctioning. Retroreflectors that would reflect the laser back to its source, could be placed around the aircraft windows as a deterrent; however, the crewmembers could still be exposed to the hazardous conditions of a laser strike within the cockpit, as well as innocent bystanders when the laser is not perfectly reflected back to the source. Also, manufacturers do not like to put additional weight onto the aircraft, or add materials that could change the aerodynamic characteristics of the aircraft. The last form of engineering control with technologies that already exist is a thin film coating applied to the aircraft windows. Thin film coatings are nanometers thick with negligible weight gains, would not change the aerodynamics of the aircraft, and can be tailored to

protect against a specific wavelength at a specific optical density. However, due to the temperatures needed during the application process, plexi-glass windows, which make up the majority of helicopter windows, could warp and deform. Thus, to continue research into developing new thin film coating application methods, this study looked at the viability of a thin film coating as an engineering control for aircraft windows and provide a baseline to compare with future studies.

The specific aims of this study compared three factors between an off-the-shelf 532nm, OD 4 notch filter (532NF) to three flat (TS 2, TS 3, and TS 4) and three curved (TS 13, TS 14, and TS 16) uncoated plexi-glass window test samples: the change in light transmission, the magnitude of glare production, and the magnitude of color distortion. Not all laser strikes occur at the same angle of incidence between the laser and the crewmember's eye; therefore, this study looked at the worst case scenario of a 00° angle of incidence and a much more likely scenario of a 60° angle of incidence.

Light transmission – Light transmission measurements were able to determine the percent loss of green light compared to the rest of the visual spectrum, the loss in radiant power, and the effectiveness of the 532NF over a range of angles of incidence. Based on the light transmission results, the 532NF does exactly what it was designed to do; reflect 532±13.3nm light down to 0.01% of the light's original absolute irradiance. However, the 532NF only performs to its specifications at or near a 00° angle of incidence to the light source. As the angle of incidence increases, the effectiveness of the 532NF decreases. The portion of the visual spectrum the 532NF is designed to reflect shifts towards the blue portion of the visual spectrum. As the notched portion of the spectrum shifts, more and more glare is produced, because more light is being allowed to transmit. This occurs because less and less thin film coating layers are properly reflecting the green light back towards the light source. Thus preventing reflective interference, which is what helps prevent more green light from transmitting. Even though the 532NF is less effective as the angle of incidence increases, the amount of light transmitting decreases. With this information, it may be possible to develop a coating that protects at higher wavelengths of the spectrum at a 00° angle of incidence with a higher OD. This way, as the angle of incidence increases, the thin film coating could properly protect against a 532nm laser above 5mW. A research study into the most common angles of incidence for laser strikes is required to help determine at which angle of incidence the notched portion of the spectrum would be needed to protect against green light.

Glare production – Glare production measurements were able to determine the change in glare magnitude produced by the laser striking the test sample. Besides the physical hazards to the eye brought on by laser exposure, glares can present a large distraction to crewmembers, especially at night

when the glare could ruin a crewmember's night vision by oversaturating the rod cells. According to the green histogram data, the 532NF was very effective in reducing the size of the glare compared to the uncoated test samples at a 00° angle of incidence; however, produced almost the same amount of glare as the uncoated test samples at a 60° angle of incidence. With the grayscale data, the 532NF was very effective in decreasing the luminous intensity of the glare produced at 00° angle of incidence as shown by its large contrast ratio when compared to the uncoated test samples; the 532NF contrast ratio was 69% higher than the Ave TS. The 532NF was also very effective in reducing the luminous intensity of the glare at a 60° angle of incidence; its contrast ratio remained 69% higher than the Ave TS. Meaning that even though the 532NF has approximately the same amount of green light transmitting and has about the same size glare as the uncoated test samples at a 60° angle of incidence, the overall luminous intensity is less than the uncoated test samples. The glare production data also suggests that there is no significant difference between the flat and curved uncoated test samples; however, there are no data on how this study's thin film coating reacts to a laser strike on a curved surface. Once a method to apply a thin film coating to plexi-glass is developed, research can be done to determine the thin film coating's effectiveness between flat and curved coated test samples and compare to the uncoated test sample data.

Color distortion – Color distortion measurements were taken because any thin film coating designed to reflect a portion of the visual spectrum will inherently become hued. Due to the narrow range of the notch ($\pm 13.3\text{nm}$) and an OD of 4.0, the 532NF had only a slight pink hue to it. Even this much color distortion, however, could have detrimental effects on the operations conducted by the USCG. USCG crewmembers depend on different colored distress signals, runway lights, and navigation lights during their missions, which may be life and death situations. The last thing a crewmember would want is this thin film coating preventing them from successfully completing their mission. According to the color distortion data, the 532NF does reflect away green light when present in the scenario; however, only reflects a noticeable amount for brighter scenarios. For the CRC, the 532NF only reflected higher intensity green light, as evident by the darkening of the green square in the left part of the CRC and the slight pink hue change to the large gray square on the right. Scenario 1 was a dark twilight scenario; thus the hue change in Figure 60 was the smallest with the 532NF. Scenario 2 was a brighter scenario, but cloudy with a dull background, so the hue change in Figure 76 was more than scenario 1's, but still barely noticeable. Scenario 3 was brighter than scenarios 1 and 2, thus the pink hue change to Figure 82 was the greatest. More research is required to determine if a thin film coating with a narrower range than $\pm 13.3\text{nm}$ could reduce the amount of color distortion.

In conclusion, results suggest that the 532NF's thin film coating is a promising start in developing a viable engineering control to protect crewmembers from the hazards of laser strikes. A $532\pm 13.3\text{nm}$, OD4, notch filter thin film coating would be able to reduce a Class 3B laser's radiant power to safe levels and produce almost no glare, if the angle of incidence is somewhere between 00° and 20° . Yet, an adjustment to the thin film coating's centered wavelength could increase the angles of incidence to which it is effective against $>5\text{mW}$, 532nm lasers.

For the thin film coating to be further effective for the USCG, it should be designed to absorb green light rather than reflect it. If the thin film coating is designed to reflect green light from entering the cockpit from outside, it will also reflect light coming from within the cockpit. Aircraft cockpits have many different lights of various colors on their instrument panels, and crewmembers would not want the thin film coating to reflect all of the 532nm wavelengths from these lights onto their windows. It may also be possible for an absorptive thin film coating to reduce glare production more than a reflective thin film coating. However, a research study would be required to quantify any change in glare production between these two types of thin film coatings.

The color distortion results suggest that the 532NF's thin film coating did not greatly reduce the visibility of the scenario. Only for brighter scenes did the 532NF reflect higher intensity green light and distort the red and blue intensity levels. Even with this small amount of distortion, the red flare and horizon in scenario 1, the lifejacket of the vessel pilot in scenario 2, and the orange smoke distress signal and personal lifejacket in scenario 3 could all be seen. However, if the USCG deems this thin film coating distorts color too much, it is possible to narrow the range of wavelengths reflected to $\leq \pm 13.3\text{nm}$ to reduce the amount of color distortion.

Lastly, there is a different type of coating, other than a thin film coating, that could absorb the 532nm light without distorting the color of the windows, called a quantum dot solution. Quantum dots are nanoparticles that can be engineered to shift the light from the visual spectrum into the infrared, thereby eliminating the hazardous conditions brought on by the laser (Qian 2011). Quantum dot solutions can also be applied to plexi-glass, because extremely high temperatures are not required during the application process, as with thin film coatings. There has been no experimentation with quantum dots as a viable means to protect crewmembers from laser strikes. Research is required to develop a quantum dots solution to absorb 532nm light and shift it to a non-visual portion of the spectrum, and compare its effectiveness to the 532NF.

VI. LIMITATIONS

One major limitation for this study was the inability of using human test subjects to determine the effectiveness of the aircraft window coatings due to the hazardous nature of laser shone on the eye. Any PPE the human test subject would need to wear during the study would skew the results. Another major limitation was determining the performance specifications needed to protect the crew from hazardous lasers strikes. Due to easy access of high intensity lasers (greater than 5mW), it is impossible to know what intensity the coating will need to protect the crew against. Only data gathered from laser strike reports published by the FAA can be used to determine the most common type of laser, which was found to be 532nm but with an unknown average intensity.

The last major limitation was not being able to test the thin film coating with green pencil flares or navigation lights onboard vessels. Green pencil flares have a thermal, chemical reaction to give off a polychromatic spectrum with green being the most prominent color, which is different to a laser that produces a monochromatic spectrum. Navigation lights onboard vessel also produce a different kind of spectrum compared to lasers. Navigation lights could be filament or led based whose primary color is green, or there could just be a green lens in front of the light source filtering out the rest of the spectrum. In both cases, the thin film coating would reflect the green portion of their spectrums, but would the crewmember still be able to clearly see the pencil flare or the navigation light without those wavelengths?

VII. ACKNOWLEDGMENTS

1. Spectrecology
 - A. Mike Morris
2. United States Coast Guard
 - A. LCDR James Cooley
 - B. LCDR David Feeney
 - C. LT Aaron Riutta
 - D. District 13 Safety and Environmental Health Office
3. University of Washington
 - A. Dr. Darick Baker
 - B. Dr. Martin Cohen
 - C. Mr. Jacob Delbridge
 - D. Ms. Amy Lim
 - E. Dr. June Spector
 - F. Dr. Mike Yost
 - G. University of Washington Field Research and Consultation Group
 - H. University of Washington Health Sciences Building Carpentry Shop

VIII. GLOSSARY

1. Absolute Irradiance – describes the absolute amount of radiant power per unit area of a surface (W/m²). By knowing the surface area of the spectrometer used in this study, the radiant power per wavelength was calculated.
2. Absorbance – describes the amount of light absorbed by a material (Gallik 2011). Absorbance can be calculated as absorbance (A) equals the minus log base 10 of transmittance (T).

$$A = -\log_{10}(T)$$

3. Beam divergence – describes the amount to which a beam of light diverges over a distance, usually in units of milliradians (mrad) for lasers (Amrita 2016). This is useful for determining the diameter of the laser beam over a distance, by using the formula beam divergence (θ) equals the difference between the final diameter in millimeters (Df) minus the initial diameter in millimeters (Di) over a distance in meters (L). The laser used in this study had a beam divergence of 1.5mrad and an initial beam diameter of 1.2mm; therefore, over a distance of 1.0m, the new beam diameter is

$$Df = (\theta * L) + Di = (1.5 * 1.0) + 1.2 = 2.7\text{mm}$$

4. Collimating Lens – used to collimate a light source, or direct the emitted light into a beam. This study called for a beam of white light transmitting through a test sample and onto the spectrometer. A 100W halogen bulb diffused light into a fiber optic cable, and traveled through a collimating lens to form a beam of white light. For a collimating lens to work, a light source must be placed at the lens’s focal point to ensure the least amount of light divergence over a distance.
5. Figure 62 illustrates an example of a collimating lens, to which the light source LD diffuses light 11.2mm away from the lens (GoFoton 2016). The designed characteristics of the lens causes the light to refract in such a way that all of the transmitting light forms into a beam.

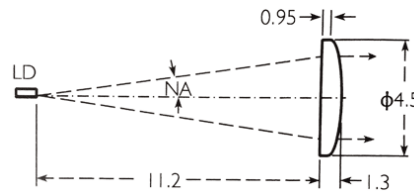


Figure 62: example of a collimating lens.

6. Critical Angle – describes the angle of incidence to which no more light transmits through a material, which causes the material to act as a mirror where all of the light is reflected off. Another term for this characteristic is total internal reflection (Nave 2016).

- Electromagnetic Spectrum – describes the energy, wavelength, and frequency of all forms of electromagnetic radiation (Cyberphysics 2016). Figure 63 illustrates the electromagnetic spectrum. This study is only interested in the visible spectrum (approximately 400nm-750nm).

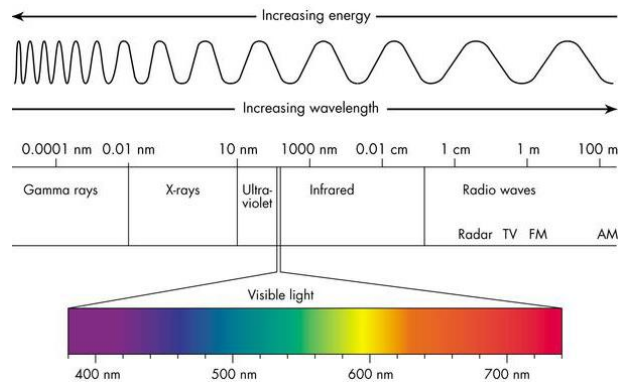


Figure 63: the electromagnetic spectrum.

- Etalon – describes the multiple reflections of light between two surfaces, causing a periodic wavelength in optical transmission measurements (Photop 2008). For this study, an etalon can be seen when the white light spectrum is measured as the WLS’s angle of attack increases with respect to the 532nm notch filter. In Figure 64, an etalon is clearly visible as a periodic wave on the right side of the graph. The number of peaks within an etalon may indicate the number of layers within the thin film coating.

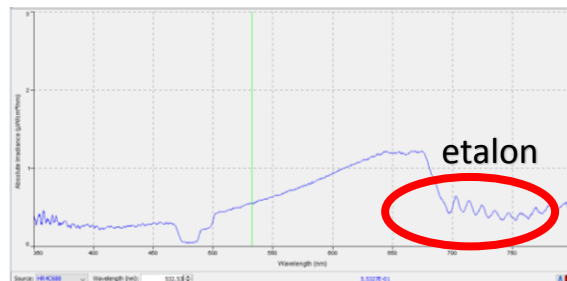


Figure 64: Absolute irradiance of the WLS onto the 532nm at 50 degrees

- Fovea – name for the central area of the macula that houses the cones cells and produces the eye’s sharpest vision (Cassin 2007). This area is most susceptible to eye damage due to laser exposures, because the eye focuses the laser’s beam into a fine point on the surface of the fovea. Figure 5 is an illustration of the eye focusing a laser beam onto the fovea. The energy of the laser’s beam may cause thermal damage on the fovea, depending on the radiant power of the laser and the duration of exposure.
- Laser – an acronym for “light amplification by stimulated emission of radiation.” A laser is a source of high energy that can emit ultraviolet, visible, or infrared light via the natural vibrations of the atoms it stimulates (Cassin 2007).

11. Light (luminous) Intensity – measurement for the visible light emitted from a source in unit per solid angle, measured in candelas or one lumen per steradian (Britannica 2016).
12. Macula – name for the small central area of the retina within the eye that surrounds the fovea (Cassin 2007).
13. Neutral Density – related to optical density, neutral density refers to the percent of light transmission for the entire visible spectrum, whereas optical density usually refers to a narrower range of wavelengths. Neutral density filters of 2.5OD and 0.9OD were used together for this study to prevent the laser light from overloading the spectrometer by only allowing 0.0398% of the 532nm light to reach the spectrometer. $(90\text{mW} * 10^{-2.5}) * 10^{-0.9} = 0.0358\text{mW}$; see Absorbance for the formula.
14. Notch Filter – a type of optical lens with a thin film coating. This type of lens is specifically designed to absorb/reflect a specific very narrow range of light wavelengths, but allow the rest of the spectrum to transmit through the lens (Reynard 2015). For this study, the notch filter was chosen to absorb/reflect a wavelength of 532nm +/- 10nm. The thin film coating was only applied on one side of the lens. The lens has an arrow along the rim indicating which way the transmitted light was allowed to travel; therefore, it is important to remember to point the arrow away from the light source.
15. Optical Density – a way to describe the percent of light transmission through a material, such as an optical filter or laser safety glasses. The percent of light transmission can be calculated by raising 10 to the power of the negative optical density number (% transmission = $10^{-\text{OD}}$). For example, the laser safety glasses used in this study had an optical density of 2 for 532nm. The percent transmission is equal to $10^{-2} * 100\% = 1\%$. Therefore, only 1% of 532nm light would be allowed to transmit through the laser safety glasses.
16. Optical Thin Film Coating – applied onto a lens to perform a desired function with regards to light transmittance and reflectance (Turner 2016). Thin film coatings may be designed as anti-reflection coatings, attenuation coatings, bandpass coatings, conductive coatings, dichroic coatings, laser protection coatings, longwave pass coatings, multi-band coatings, shortwave pass coatings, ultraviolet coatings, infrared coatings, visible coatings, and more (Reynard 2015). Each type of thin film coating has a specific layering formula to produce the desired effect, and can be anywhere from four layers to a couple thousand layers with each layer being nanometers thick. Thin film coatings can be applied in a variety of methods each having their own advantages and disadvantages, such as thermal evaporation deposition, ion-beam sputtering, ion-assisted

deposition, magnetron sputtering, chemical vapor deposition, or more (Turner 2016). The 532nm notch filter used in this study was designed to absorb/reflect 532nm light, but allow the rest of the visible spectrum to transmit through the lens. However, further details on how the 532nm notch filter does this is limited, because the layering formula and application process are proprietary to the manufacturer.

17. Radiant Power – measurement for the amount of light emitted from a source per second, measured in lumens (Britannica 2016).
18. Retina – name of the light sensitive nerve tissue within the eye (Cassin 2007). The retina transforms the images captured by the eye into electrical signals, which are then translated by the brain.
19. Spectrometer – a device designed to measure the properties of detected light (Pembroke 2013). Figure 65 illustrates how a UV-VIS spectrometer detects light, such as the spectrometer used for this study. The detectable light is transmitted through or reflected off a material, travels through focusing optics, is diffracted by a grating which acts as a prism, and is read by a sensor. The sensor has a very small slit that allows the diffracted light to enter, and where the light hits the sensor determines its wavelength. Usually, spectrometers only measure the intensity of light per wavelength, but for this study the spectrometer was fitted with a cosine corrector allowing for the spectrometer to also measure light power and other light properties.

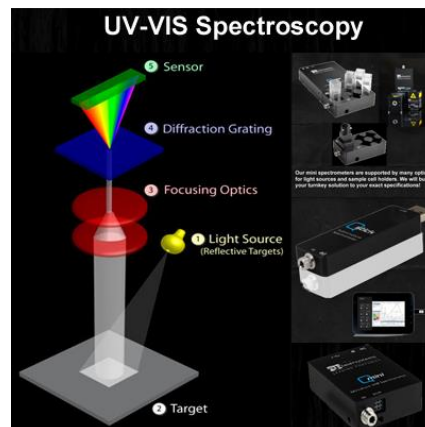


Figure 65: illustration of how a spectrometer detects the properties of the detectable light.

20. Transmittance – describes the percentage of all light that travels through a material (Gallik 2011). Transmittance can be calculated as transmittance (T) equals the intensity of the transmitted light (I_o) divided by the intensity of the incident light (I).

$$T = I_o/I$$

IX. REFERENCES

1. American National Standards Institute. 2014. ANSI Z136.1-2014 – Safe Use of Lasers.
2. Amrita University. 2016. Laser beam divergence and spot size. Retrieved from: <http://vlab.amrita.edu/?sub=1&brch=189&sim=342&cnt=1>.
3. Bush E. October 2015. 2 ferry workers injured by laser fired into boat near Mukilteo. The Seattle Times. Retrieved from: <http://www.seattletimes.com/seattle-news/transportation/2-ferry-workers-injured-by-laser-fired-into-boat-near-mukilteo/>.
4. Cassin B. 2007. Glossary of Eye Terminology. Retrieved from: <http://www.eyeglossary.net/>.
5. Cyberphysics. 2016. The Electromagnetic Spectrum: the family of Light. Retrieved from: <http://www.cyberphysics.co.uk/topics/light/emspect.htm>.
6. Derenski P. 2010. Reducing the Threat of Laser Illuminations. Boeing, AERO QTR_01.10. Retrieved from http://www.boeing.com/commercial/aeromagazine/articles/qtr_01_10/3/.
7. Encyclopedia Britannica. 2016. Luminous Intensity: Physics. Retrieved from: <http://www.britannica.com/science/luminous-intensity>.
8. Gallik S. 2011. Transmittance and Absorbance. Cellbiology OLM. Retrieved from: <http://cellbiologyolm.stevegallik.org/node/7>.
9. Gilley C. July 2015. Can someone on the ground really endanger an aircraft using a laser pointer? Quora. Retrieved from: <https://www.quora.com/Can-someone-on-the-ground-really-endanger-an-aircraft-using-a-laser-pointer>.
10. GoFoton. 2016. SELFOC Laser Diode Collimating Lenses. Retrieved from: https://welcome.gofoton.com/product/collimating_lenses/.
11. Kravets D. November 2014. Laser strikes force US Coast Guard helicopter missions to abort. Arstechnica: Law and Disorder/Civilization and Discontents. Retrieved from: <http://arstechnica.com/tech-policy/2014/11/laser-strikes-force-us-coast-guard-helicopter-missions-to-abort/>.
12. LaserFX. 2008. Basic Laser Safety – Eye and Skin Hazards. Retrieved from: <http://www.laserfx.com/BasicSafety/BasicSafety2.html>.
13. Lee G, Baurnal C, Lally D, Pitcher J, Vander J, Duker J. 2014. Retinal Injury After Inadvertent Handheld Laser Exposure. Retina, The Journal of Retinal and Vitreous Diseases. 34:12, 2388-2396.
14. Marshall J, O'Hagan J, Tyrer J. April 2016. Eye hazards of laser 'pointer' in perspective. Br J Ophthalmol. Retrieved from: <http://bjo.bmj.com/>.
15. Moreno J. April 2015. Coast Guard helicopter hit by laser strike in Port Angeles. KOMO News. Retrieved from: <http://www.komonews.com/news/local/Coast-Guard-helicopter-hit-with-laser-pointer-in-Port-Angeles-300880721.html>.
16. Nakagawara V, Montgomery R, Wood K. November 2011. Laser Illumination of Flight Crewmember by Altitude and Chronology of Occurrence. Aviation, Space, and Environmental Medicine. 82:11 1055-1060.

Assessing Potential Laser Strike Protection Engineering Control for United States Coast Guard Aircraft

17. Nave R. 2016. Total Internal Reflection. Hyperphysics. Retrieved from: <http://hyperphysics.phy-astr.gsu.edu/hbase/phyopt/totint.html>.
18. Negroni C. December 2013. The Laser Threat: Authorities struggle to shut off beams aimed into cockpits. Air and Space Magazine. Retrieved from: <http://www.airspacemag.com/flight-today/the-laser-threat-180947755/?no-ist>.
19. Pembroke Instruments. 2013. How a Spectrometer Works. Retrieved from: <http://pembrokeinstruments.com/spectrometer-how-it-works/>
20. Photop. 2008. Etalon. Retrieved from: http://www.photoptech.com/main/products_gx/pdf/Telecom%20Optics/Etalon/Etalon.pdf
21. Qian L, Zheng Y, Jiangeng X, Holloway P. 2011. Stable and efficient quantum-dot light-emitting diodes based on solution-processed multilayer structures. Nature photonics. 5, 543-548
22. Reynard Corporation. 2015. Thin Film Coatings: Custom. Retrieved from: <http://www.reynardcorp.com/optical-production-capabilities/thin-film-coatings-custom.html>
23. Stangroom J. 2016. Social Science Statistics. P Value from T Score Calculator. Retrieved from: <http://www.socscistatistics.com/pvalues/tdistribution.aspx>.
24. Thewlis M. April 2014. How do we perceive colour? Retrieved from: <http://littlewebgiants.com/how-do-we-perceive-colour/>.
25. Turner T, Kirshner R. 2016. Thin-Film Coatings: A Buyers' Guide. Retrieved from: <http://www.photonics.com/EDU/Handbook.aspx?AID=42399>
26. University of New Mexico. Human Cone Action Spectra. Retrieved from: https://www.unm.edu/~toolson/human_cone_response.htm.
27. US Coast Guard. 2014. Aviation Safety Annual Report: Fiscal Year 2013.
28. US Federal Aviation Administration. February 2014. Fact Sheet – Laser Strikes. Retrieved from: https://www.faa.gov/news/fact_sheets/news_story.cfm?newsId=15774.
29. US Federal Aviation Administration. November 2015. Laser Pointer Safety – Statistics, laws, and general laser pointer news. Retrieved from: http://www.laserpointersafety.com/news/news/other-news_files/tag-faa.php.
30. US Food and Drug Administration. December 2010. FDA Safety Notification: Risk of Eye and Skin Injuries from High-powered, Hand-held Laser Used for Pointing or Entertainment. Retrieved from: <http://www.fda.gov/MedicalDevices/Safety/AlertsandNotices/ucm237129.htm>.
31. US Occupational Safety and Health Administration. Laser Hazards. OSHA Technical Manual Section III: Chapter 6. Retrieved from: https://www.osha.gov/dts/osta/otm/otm_iii/otm_iii_6.html#3.
32. Wyrsh S, Baenninger P, Schmid M. September 2010. Retinal Injuries from a Handheld Laser Pointer. The New England Journal of Medicine. 363:11, 1089-1091.

X. APPENDIXES

- A. Lens Cleaning Procedures
- B. Methods Procedures
- C. Laser Lab Safety Procedures
- D. Spectrecology spectrometer Procedures
- E. Additional Results